Immunoassay Sensitivity and Kinetic Enhancement in Cell Culture Media using Electrokinetic Preconcentration

by

Leon Daliang Li

B.S., Electrical Engineering (2006)
University of Pittsburgh

Submitted to the Department of Electrical Engineering
in Partial Fulfillment of the Requirements for the Degree of
Master of Science in Electrical Engineering

at the
Massachusetts Institute of Technology
February 2009

Signature of Author _____
Department of Electrical Engineering
January 21, 2009

Certified by _____
Jongyoon Han
Associate Professor of Biological Engineering
Thesis Supervisor

Accepted by _____
Terry P. Orlando
Chairman, Department Committee on Graduate Students

Abstract

The microfluidic cell culture enables the study of cell signaling in previously impossible or impractical ways by allowing the precise spatial and temporal control of the microenvironment to better mimic *in vivo* conditions. Microfluidic techniques allow the creation of exact culture geometries, cell patterns, and the use of perfusion techniques to precisely control external soluble factor signaling and effectively inhibit autocrine signaling factors. To date, microfluidic techniques have been used to perform single-cell analyses, generate molecular gradients, and pattern three-dimensional cultures.

The task of identifying and quantifying the cell culture proteome from cell lysate or the secreted proteins is often performed by the immunoassay. Macroscale immunoassays such as those performed on the tissue culture plate, however, are of limited use for the microfluidic cell culture due to the limited volume of sample generated by the microfluidic culture. The ability to precisely patterning cells on the microscale (10-100um) enables cell study at physiological length scales, but also drastically reduces both the sample volume and the protein abundance when compared to the tissue culture plate. Due to these twin challenges of low sample volume and low secreted protein concentration, the detection of protein antigens by immunoassay on many microfluidic cell cultures applications is currently practically infeasible.

To address the limitations of low sample volume and low protein concentration, we have developed a novel microscale immunoassay device capable of the electrokinetic concentration of proteins. This technique allows us to improve the sensitivity of immunoassays through increasing the antigen concentration prior to antibody-antigen binding, or preconcentration. Using this scheme, we have demonstrated a 100 fold sensitivity improvement for antigens directly from cell media without sample preparation when compared with immunoassays without preconcentration. Our immunoassay also benefits from sub microliter required sample volume and may be easily integrated directly to microfluidic cell cultures.

Furthermore, we fabricated microelectrodes integrated on chip to the electrokinetic preconcentrator to directly measure the electric field which accompanies nonlinear electrokinetic flow. The time response electrical profiles of electrokinetic preconcentration was obtained and correlated to the protein concentration profile to study electrokinetic behavior. Our efforts yielded a method to directly visualize the electric field distribution in nonlinear electrokinetic flow and a direct relationship between the depletion effects of electrokinetic behavior and the electric field profile.

Table of Contents

Chapter 1: General Immunoassay Principles and Applications to Biosensing

The immunoassay is one of the most commonly used methods in biology to measure the presence or concentration of a biomolecule in a simple such as serum or cell culture media. The assay makes use of the highly specific binding between the antibody and antigen. This provides a method to reproducibly identify and quantify the presence of antigen if an appropriate antibody can be reliably produced in the lab.

Antibodies are "Y" shaped soluble protein produced by the immune system of vertebrates and are found in serum and other bodily fluids. The tips of the Y consist of antigen binding protein fragments (Fab region). In most cases, the Fab region binds to a specific section or epitope of the appropriate antigen molecule, analogous to what is usually described as a lock-and-key mechanism. The base of the Y is the crystallizable fragment (Fc region), whose function is to modulate immune cell activity. Antibodies protect the organism against foreign invasion through several methods. Antibody binding may interfere with the function of an antigen protein through steric hindrance, or by inducing conformation change. The Fc region of a bound antibody also triggers subsequent reactions and immune system cascades to activate complement defenses or effector cells.

The unique requirements and properties of the antibody mediated immune response make the antibody-antigen reaction an excellent tool to detect and measure biomolecules in a complex biosample. Blood serum is a complex mixture of dissolved ions, proteins, sugars, lipids, and other components. Even within this complex environment, the Fab region is capable of recognizing an essentially unlimited combination of biomolecules while the constant Fc region allows for chemical attachment to solid supports and subsequent signal transduction without affecting the antibody's binding affinity.

Antibodies for immunoassays are produced through inoculating an animal with antigens followed by harvesting of the antibodies from the animal's serum. (1) Antibodies produced this way are called polyclonal and are antigen specific but are targeted to different epitopes. Monoclonal antibodies, or those directed against a single epitopes, can be created by isolating and immortalizing a single epitope targeting B-cell clone.(2) Since polyclonal antibodies target multiple epitopes, polyclonal antibodies are

more robust and resistant to operating conditions such as pH and ionic strength but exhibit greater batch-to-batch variation, while monoclonal antibodies are in general more specific but less robust.

Enzyme-Linked ImmunoSorbent Assay (ELISA)

The Enzyme-Linked ImmunoSorbent Assay, or ELISA, is the most commonly used immunoassay. The "sandwich" assay form of ELISA is diagramed in Figure 1. First, capture antibodies are immobilized onto a solid support, such a polystyrene plate or a microbead. Multiple chemistries are available for this process, such as nonspecific adsorption, protein A attachment, and streptavidin-biotin interaction. The immobilized antibody is then incubated with the sample and a secondary antibody. Antigens specific to the antibodies used will be "sandwiched" between the capture and secondary antibodies. To minimize the nonspecific absorption of antigens, blocking molecules such as bovine serum albumin or TWEEN 20 are usually added. The secondary antibodies are conjugated to a specially chosen reporter molecule, such as an enzyme to change color or produce fluorescence. The plate or beads are then washed to remove excess reagents, and the appropriate enzyme substrate is added. The enzyme substrate reaction produces a detectable change after multiple reaction cycles. The enzyme substrate reaction can be quantized and correlated to the concentration of antigen molecules in the original sample.

The secondary antibodies' enzyme label can be easily replaced with other reporter molecules, such as a chemiluminescent compound, cofactor such as ATP, or electroactive compound. The choice depends mostly on the sensitivity required and the needs of the application. For ELISAs in the clinical diagnosis setting, the most common choice is the horseradish peroxidase (HRP) enzyme, which reacts with many substrates to generate hydrogen peroxide as an oxidizing agent to drive a color change. Figure 2 shows an example of HRP generated color change in HIV testing.

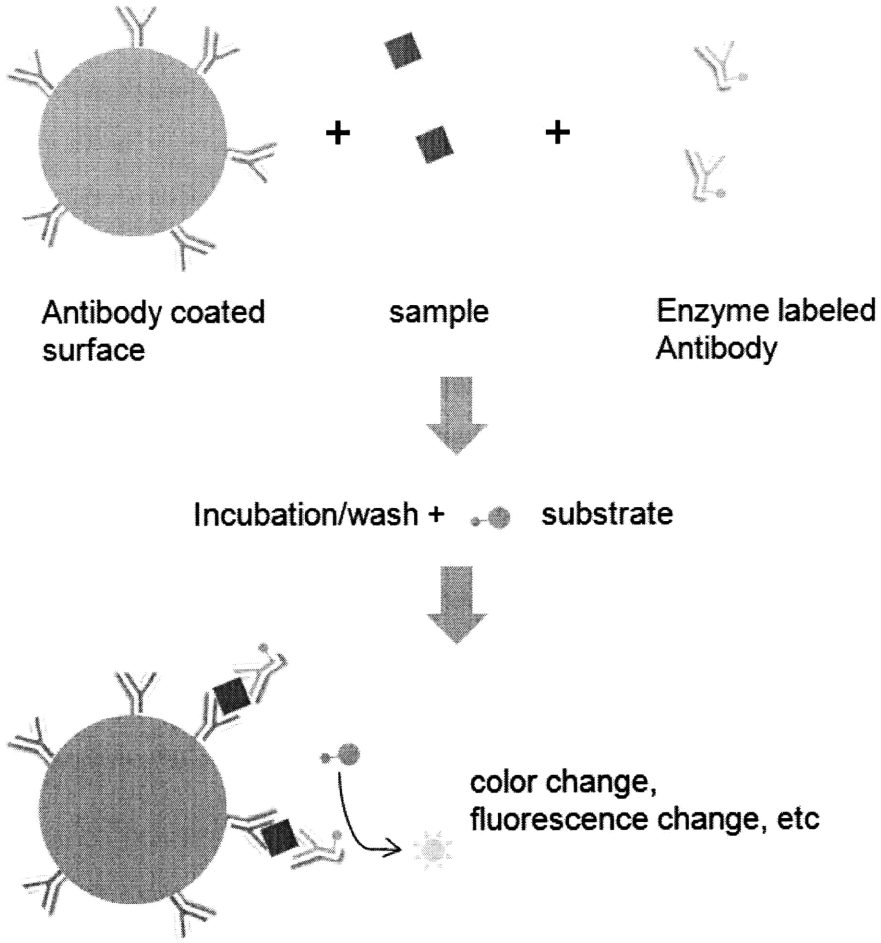

Figure 1: Enzyme-Linked ImmunoSorbent Assay (ELISA) for the detection of a specific antigen.

The ELISA benefits from high specificity. This is particularly true in the case of the two-antibody sandwich assay just described, as each antibody may compensate for any nonspecific binding from the other one. The primary drawback is the limitation of the antibody-antigen binding kinetics and the mass transport limitation of the assay. The sensitivity of the microwell plate based ELISA is usually in the picomolar to nanomolar range, although special amplification techniques can be used to achieve much femtomolar sensitivities. Most current ELISAs require a minimum sample volume of 50µL.

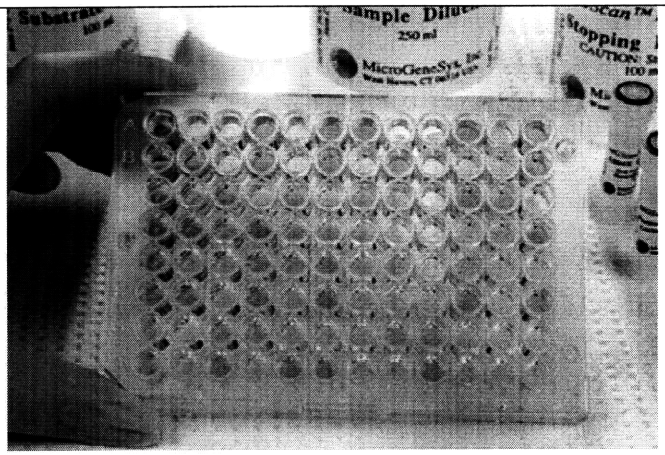

Figure 2: HIV testing using ELISA on a 96-well plate. The brown color results from activity by the secondary antibody's conjugated horseradish peroxidase and indicates the presence of HIV infection in the sample.

The sensitivity of immunoassays is also adversely affected by the amount of background noise. Figure 3 shows the sources of background noise in immunoassays, which includes electronic noise, assay reagent blank, and non-specific binding. (3) On microfluidic assays, non-specific binding is particularly problematic due the larger surface area to volume ratio. Most high sensitivity assay designs are created to reduce one or more of these noises, or to increase the detection signal through various amplification strategies. For example, the enzyme conjugation in ELISA provides post-binding amplification in the assay, as each the enzyme bound to each captured antigen reacts with multiple substrate molecules. Non-specific binding with heterophilic antibodies (directed against proteins from a different species) and auto-antibodies (such as rheumatoid factor) in blood is a cause of both false positives and false negatives in immunoassays. (4) The approach to this problem has been the addition of factors such as animal serum or specific proteins with high antibody affinity to neutralize the interfering antibodies. (5)

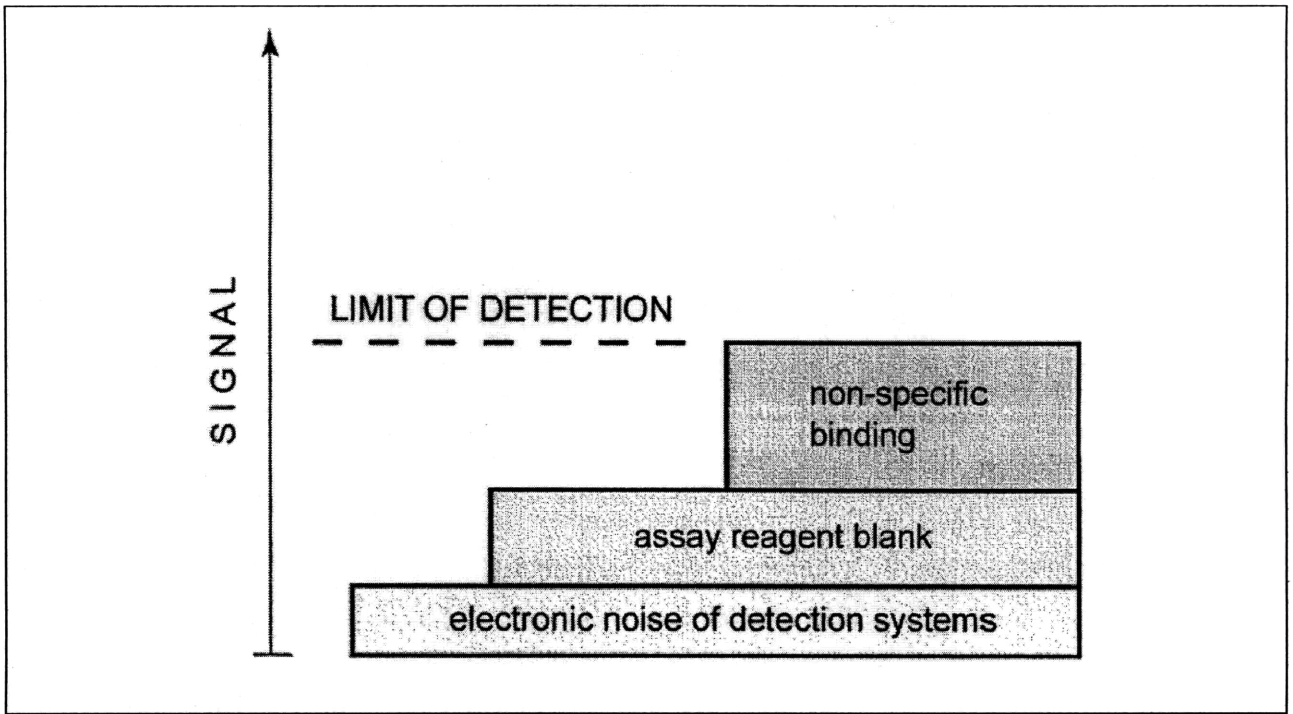

Figure 3: Sources of background noise in immunoassays. (3)

Kinetics of Immunoassays and Limitations

Antibody-antigen reaction kinetics are reversible and governed by the Law of Mass Action. In solution, the reaction is

$$[\mathrm{Ag}]+[\mathrm{Ab}] \leftrightarrow [\mathrm{AgAb}] \qquad (1)$$

where [Ag] is the antigen concentration, [Ab] is the antigen concentration, and [AgAb] is the bound antibody-antigen complex concentration. By the Law of Mass Action, the rate of accumulation for the bound complex is given by

$$\frac{d[\mathrm{AgAb}]}{dt} = k_f[\mathrm{Ag}][\mathrm{Ab}] - k_r[\mathrm{AgAb}] \qquad (2)$$

where k_f is the forward rate, and k_r is the reverse rate. The reaction reaches equilibrium when the forward reaction equals the reverse reaction, and can be found by setting the accumulation rate to zero:

$$K = \frac{k_f}{k_r} = \frac{[\mathrm{AgAb}]}{[\mathrm{Ag}][\mathrm{Ab}]} \quad (3)$$

Expectedly, these equations indicate that the accumulation rate is strongly dependent on the antigen and antibody concentrations. The minimum detectable concentrations or sensitivity of any immunoassay depends on the concentration of the antibody-antigen complex, and the time required for detection depends on the rate of reaction. As the antigen concentration drops, so does the equilibrium complex concentration (equation (1)) and rate of accumulation (equation (2)). Therefore, the detection of very low concentration antigens is particularly challenging, since the rate of complex accumulation would be very low and the maximum complex concentration given by the equilibrium reaction may also be too low to be detected.

Most immunoassays, such as the ELISA, are heterogeneous assays, where the antibody or the antigen (less frequently) is immobilized onto a solid surface rather than in solution. The equations above are only approximately correct in these cases because of the presence of a diffusion boundary layer. Shown in Figure 4, antigens close to the wall react with the immobilized antibodies, resulting in a diffusion layer near the wall with a lower concentration of antigens than in the bulk solution. The diffusion layer hinders formation of the bound antigen-antibody complex, since antigens must diffuse across the boundary to bind with the immobilized antibodies. Convection can reduce the width of the diffusion layer, but cannot eliminate it because of the no-slip condition at the wall.

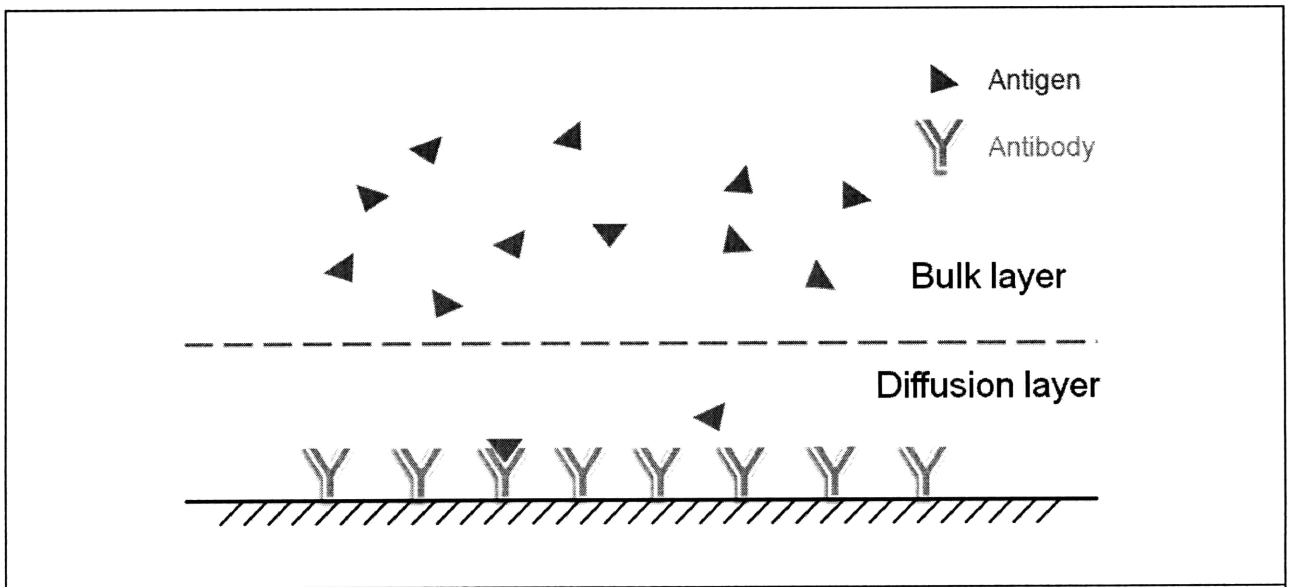

Figure 4: Diffusion layer in heterogeneous immunoassays. Antigens must diffuse across a diffusion layer before

reacting with antibody. The width of the diffusion layer is higher for lower antigen concentrations.

The time response of a heterogeneous assay with fixed antibodies can be studied by considering equation (2) with the following convection diffusion equation

$$\frac{\partial[\mathrm{Ag}]}{\partial t} + \mathbf{u} \cdot [\mathrm{Ag}] = D\nabla^2[\mathrm{Ag}] \tag{4}$$

where $\mathbf{u}$ is the velocity vector and D is the antigen's diffusion constant. Nair et. al. (6) estimated the performance limits of immunoassays based on these equations and arrived at

$$t_c < \frac{N_s r}{D[\mathrm{Ag}]} \tag{5}$$

where t_c is the minimum incubation time needed to capture the N_s minimum number of molecules needed to achieve detection, and r is the effective radius of the sensor. N_s is mostly determined by the immunoassay technology's signal transduction method (optical, impedance change, etc), and r is an argument for miniaturization of the sensor. For a given incubation time and antigen concentration, the rate limiting step is the diffusion rate of the antigen rather than the reaction kinetics. (6,7) For this reason, high sensitivity ELISAs are often incubated for many hours to days. As the antigen concentration decreases, the incubation time required quickly becomes impractically large. (7-9)

Microfluidic Cell Cultures and Immunoassays

The recent decade has seen the development of the microfluidic cell culture, driven by deficiencies of the petri dish cell culture. Because the petri disk is inherently a 2D environment, plated cells often form a monolayer on the bottom of the dish and form morphologies quite different from *in vivo* tissue structures. (10) For example, the extracellular matrix in known to affect chromatin structure and thereby gene expression in mammary epithelial cell lines (11) The dichotomy between 2D and environment is thought to be due to differences in cell-cell signaling and cell-environment interactions. *In vivo* studies on chick embryos show that the fate of individual cells during development do not rely on just gene expression patterns but take developmental cues from their positions and mechanical forces. (12) The influence of mechanical forces is also seen in the zebrafish, where large shear forces from blow flow are needed for proper heart development. (13) The microfluidic cell culture addresses many of the petri dish's shortcomings. Controlling the flow rate or perfusion sets the desired shear forces and allows

the separation of autocrine signaling from external signaling by soluble ligands. (14) Furthermore, the 10 to 100μm length scale of microfluidic channels approximates physiological cell length scales and enables the study of precise cell-cell signaling and cell-environment interactions. (15)

Microwell plate based immunoassay such as the ELISA is generally unsuitable for microfluidic cell cultures. First, the sample volume available is too small for most plate immunoassays. Also, the microfluidic cultures study a relatively small number of cells under flow perfusion. In contrast, the petri dish cell cultures study a large number of cells in static media. As a result, higher sensitivity immunoassays are often required for microfluidic cultures. Furthermore, the autocrine or paracrine signaling ligands used by cells are usually secreted in tiny quantities. Secretion of TGF-beta by mESCs, for example, clocks in at 1ng per 24 hours by 1 million cells. (16). The stringent requirements call for microfluidic immunoassays to be directly coupled to the cell culture to achieve minimal sample waste and amplification techniques to achieve high sensitivity.

Current Microfluidic Immunosensing Methods

The current gold standard in microfluidic immunoassays is immunosensing by flow cytometry, mostly performed by Luminex Corporation. In this technology, microbeads functionalized with capture antibodies are incubated together with the sample and a secondary labeled antibody in solution. The beads are then washed and sent through a flow cytometer. Inside the instrument, hydrodynamic focusing passes single beads through a section of the channel undergoing laser excitation, causing the bead and secondary antibody label to fluoresce. A fluorescence detector reads the emitted fluorescence to determine whether antigens are captured on the bead and thus present in the original sample. (17) By varying the composition of the bead, label of the secondary antibody, and using multi-wavelength lasers and detectors, immunosensing by flow cytometry can be used to simultaneously quantify up to 100 antigens with a detection sensitivity as low as 1pg/ml. (Luminex xMap Platform, (18))

Imunosensing by flow cytometry has inherent multiplexing power, since the only challenge between implementing the assay to detect one antigen and multiple antigens is in engineering the labels and optics. Furthermore, the antibodies can easily be readily by other molecules, such as oligonucleotides and lipid receptors. As a result, it is often used to obtain protein expression profiles or genotype single nucleotide polymorphism. (19) The primary disadvantage is that the incubation step requires a 40μL

sample volume, beyond the range of many microfluidic studies. Direct integration of cell cultures to the technology is also mostly impractical, since the expensive and bulky flow cytometer is usually accessible only as an off-site service rather than in-house technology in most research labs.

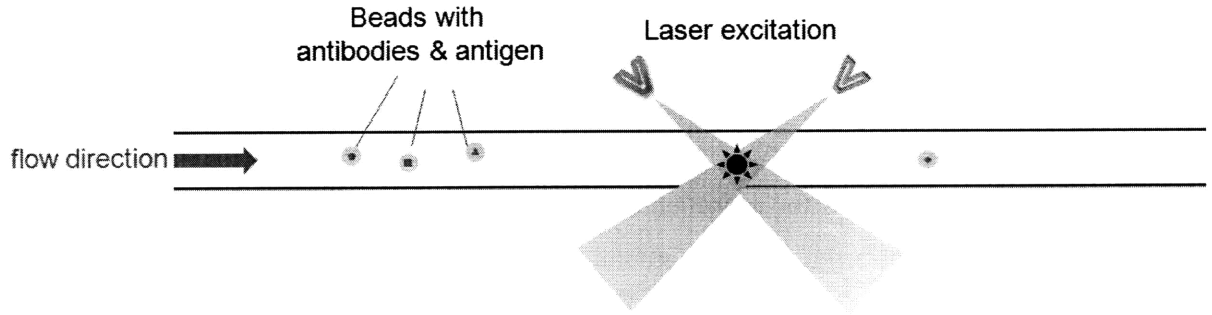

Figure 5: Diagram of microfluidic immunosensing by flow cytometry. Beads functionalized with capture antibodies are incubated with the sample and label secondary antibodies. These beads are then fed into a cytometer and interrogated with laser excitation. Multiplexing is achieved through using multiple bead compositions, antibodies labels, and multiple wavelength lasers.

Sensitivity Improvement by Post-binding Amplification

Postbinding amplification increases the signal to noise ratio of the immunoassay through chemical or biological techniques performed after the antibody-antigen reaction. The most common technique, presented in an earlier section, is the use of an enzyme labeled secondary antibody which reacts with multiple substrate molecules for each binding event. Extending this technique to multiple steps leads to additional amplification, where the first enzyme-substrate reaction produces a product which amplifies a subsequent detection reaction. Using this method, a 100-fold improvement in sensitivity has been demonstrated. (20) The technique of using multiple enzyme amplification steps has been used to quantify extremely low protein concentrations. For example, the acetate kinase enzyme has been used to convert ADP to ATP to drive the fire fly's luciferin protein into fluorescing and quantify acetate kinase in the zeptomolar concentration range. (21)

The most impressive post binding amplification techniques developed to date is amplification by PCR, where the antibody-antigen reaction leads to the release of short reporter DNA sequences which can be amplified through PCR. Figure 6 diagrams the use of a liposome/DNA mediated immunoassay. Samples urine containing CTBS and liposomes functionalized with a lipid receptor specific to CTBS is incubated

over a glass slide functionalized with CTBS capture antibodies. After washing the slide, DNAse is added to remove any nonspecifically bound DNA present in the sample and then denatured by heating the slide. The reporter DNA encapsulated inside the liposome is then released by chemically degrading the liposome membrane, followed by quantification of the reporter DNA by real time polymerase chain reaction (PCR). The achieved sensitivity was 0.75fg/ml (377 molecules) in farm runoff samples and 0.09fg/ml (43 molecules) in urine samples. In this case, cholera toxin beta subunit (CTBS) is the antigen under assay, although the technique can be readily adapted to a general immunoassay. (22)

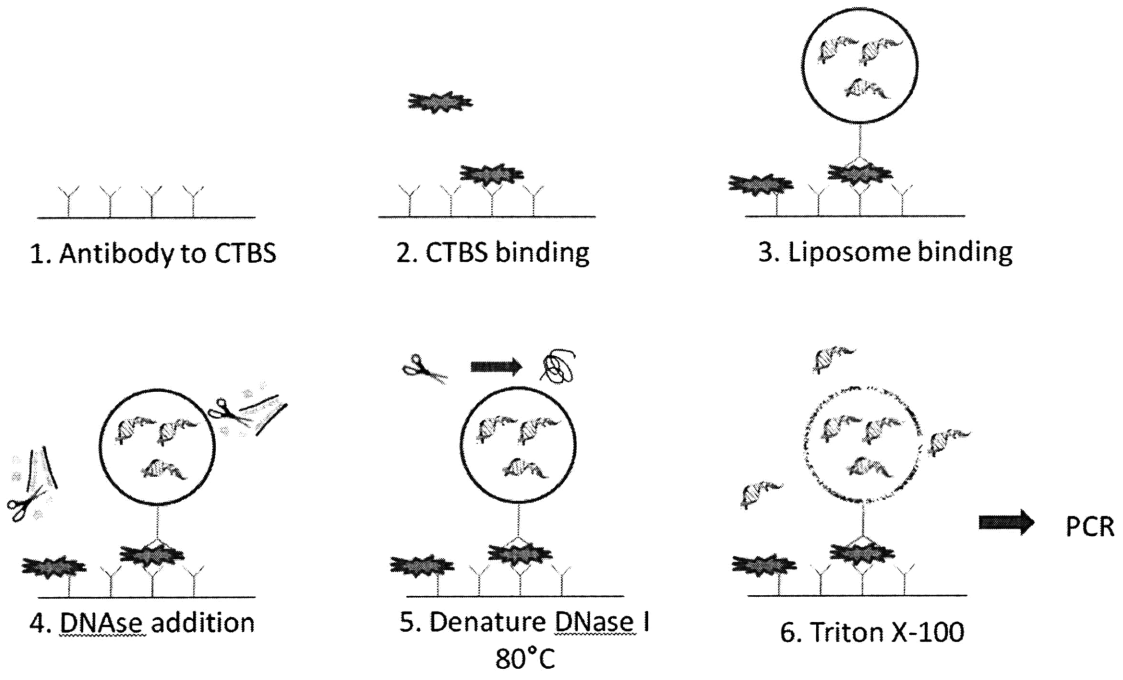

Figure 6: Diagram of liposome-PCR immunoassay to quantify cholera toxin beta subunit (CTBS). 1-3. The CTBS toxin is sandwiched between anti-CTBS and a liposome containing reporter DNA. 4-5. DNAse is added to destroy any stray DNA in the sample. 6. The surfactant Triton X-100 is added to degrade the liposome membrane, and real time PCR is used to quantify the reporter DNA released. (22)

Nam *et. al.* devised a similar sandwich assay with a nanoparticle probe. Microbeads functionalized with capture antibody and nanoparticles functionalized with both the secondary antibody and reporter DNA sequences are incubated with the sample, resulting in microbead-antigen-nanoparticle complexes. After washing to remove unbound nanoparticles, the reporter DNA sequences on the bound

nanoparticles are be released and identified with PCR. The sensitivity after PCR is 3 attomolars, and multiplexing can be achieved easily by using beads functionalized with different antibodies and DNA segments. (23)

Despite very impressive sensitivities, PCR strategies have largely not been miniaturized successfully to microfluidic formats, mostly since microfluidic PCR is not yet reliable.

Sensitivity Improvement by Sensor Miniaturization and Improved Signal Transduction

The sensitivity can also be improved by novel signal transduction capabilities. Kurita et. al. created a two stage competitive microfluidic immunoassay based on surface plasmon resonance (SPR). The biological sample is first reacted with an enzyme conjugated antibody in known excess concentration. The remaining unbound antibody is reacted with the substrate. The enzyme reaction produces a thiol product that binds to a gold surface downstream, resulting in an angle change in the SPR output signal. Picomolar sensitivity was achieved, but a potential drawback is the difficulty in selecting a proper excess antibody concentration if the antigen order of magnitude is unknown. [7] SPR is the current gold standard for determining binding kinetics and is being developed in the microfluidic form. (24)

In microcantilevers designs, antigen binding to an antibody functionalized cantilever changes the cantilever's deflection or resonant frequency. (25) (26) Femtomolar sensitivity can be achieved. Unlike most immunoassays, microcantilevers assays do not require optical detection but need sensitive electronics. Smaller devices lead to higher sensitivity since the relative impact of a single binding event increases as the sensor size decreases. The current limit for this miniaturization process is the nanowire sensor, where silicon nanowire transistors are modified into immunoassays through the chemical attachment of capture antibodies. (27) The nanowire conductance changes upon antigen binding, with reported detection sensitivity range also in the femtomolars. Multiplexing capability was achieved through the attachment of multiple antibodies to multiple nanowires.

Chapter 2: Sensitivity Improvement through Prebinding Concentration

Post-binding amplification strategies can lead to very impressive detection sensitivities. In general, posting binding amplification seeks to achieve high sensitivity by amplifying a small number of antibody-antigen binding events. These strategies, however, cannot address the diffusion limited nature of mass transport in high sensitivity immunoassays. Figure 7 illustrates this diffusion limited nature by showing

the binding dynamics of R-Phycoerythrin (RPe) obtained using a bead based microfluidic immunoassay. Microbeads were functionalized with anti-RPe antibodies, immobilized inside a microfluidic channel, and incubated with the sample under a high flow rate (>1mm/s, 1μl/min). (The experimental setup is presented in more details in the next chapter.) At RPe concentrations above 1μg/ml, equilibrium was rapidly achieved within 10 minutes. However, at lower concentrations, equilibrium was not achieved during the 60 minute experiment. These results indicate that in spite of the high convection rate, the antibody-antigen binding kinetics results in a diffusion limit mass transport regime for immunoassays detecting a sample concentration of RPe less than 1μg/ml. Figure 7 also clearly shows that increasing the incubation time from 30 minutes to 60 minutes only marginally improved the detection result, despite consuming an additional 30μl of sample.

A

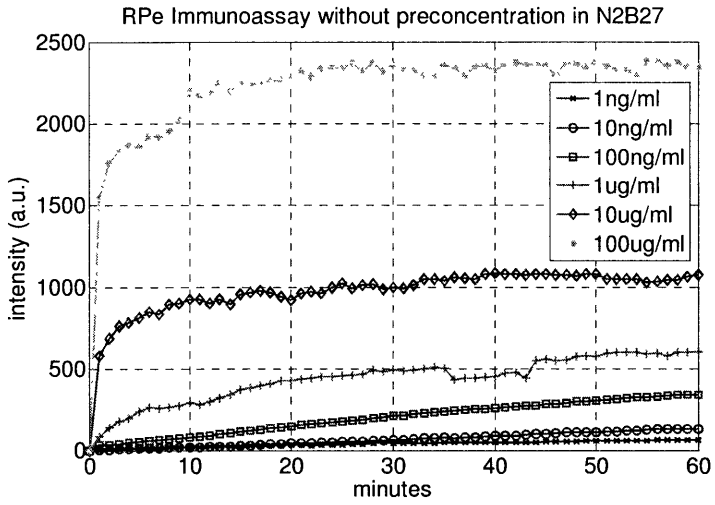
RPe Immunoassay without preconcentration in N2B27
intensity (a.u.)
minutes
1ng/ml
10ng/ml
100ng/ml
1ug/ml
10ug/ml
100ug/ml

B

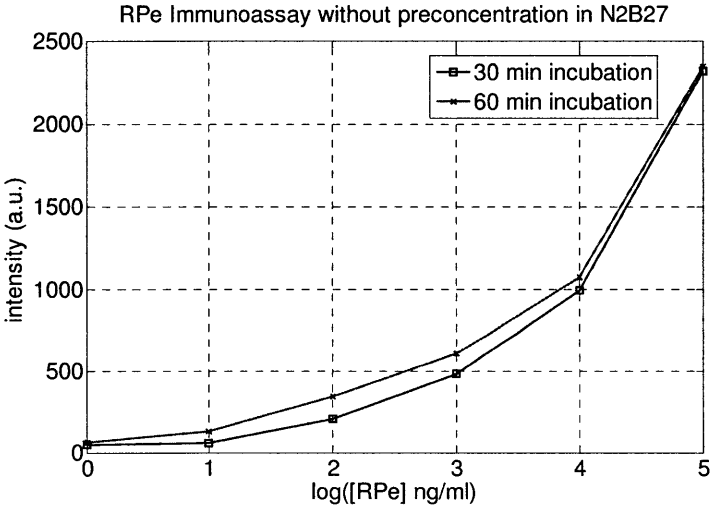
RPe Immunoassay without preconcentration in N2B27
intensity (a.u.)
log([RPe] ng/ml)
30 min incubation
60 min incubation

Figure 7: Microfluidic immunoassay without preconcentration performed inside the immunoassay without prebinding amplification. Microbeads were functionalized with anti-RPe antibodies and incubated with N2B27 media spiked with RPe under a 1mm/s perfusion rate inside the microfluidic channel. The intensity of the bead correlates to the amount of RPe captured. A: At the RPe concentration decreases below 100ng/ml, the rate of RPe binding decreases significantly due to the limitations of antibody-antigen binding kinetics. B: Increasing the incubation time from 30 minutes to 60 minutes only marginally improved immunoassay performance, suggesting longer incubation will not lead to significant increase in sensitivity.

Wang *et. al.* demonstrated an prebinding amplification strategy for immunoassays to detect RPe by electrokinetically preconcentrating the antigen molecules and achieved a 1000 fold sensitivity improvement. (28) Unlike post amplification where the strategy is to maximize the signal from each binding event, prebinding amplification seeks to increase the number of binding events by increasing the concentration of antigen molecules near the capture antibody. The higher antigen concentration shifts the immunoassay into more favorable binding dynamics, with a higher equilibrium binding concentration and lower incubation time.

A variety of techniques have been developed to increase the local concentration of antigens. Solid phase extraction uses affinity, electrostatic, or other nonspecific forces to bind analyte to a solid surface, followed by the introduction of a second buffer to elute the concentrated samples. The maximum concentration factor is approximately 1000. (29) Isoelectric focusing (IEF) is primarily a method to separate proteins by their pI value, or isoelectric point. (30) Sample proteins in a channel electrophoretically migrate down a pH gradient and pile up at the pH value equal to its pI. Field amplified sample stacking (31) and isotachophoresis (32) creates two or more regions of differing conductivities. Since the flow speed of charged analytes depends on the electric field strength, changes in electric field strength at the region interfaces creates analytes flow "bottlenecks" and concentration plugs. Furthermore, the locations of these concentration plugs depend on the electrophoretic mobility of the ion in question, allowing the separation of ions by mobility. All these techniques, however, require the use of special buffers, limiting their integration capability.

Preconcentration using Electrokinetic Trapping

Electrokinetic trapping's principle of operation is based on the depletion and enrichment effects which accompany charge selective transport. The electrolyte concentration profile near a (cation) charge

selective membrane is shown in Figure 8. Under an applied electric field, (positive) counter ions are preferentially transported across the membrane. According to classical concentration polarization theory, (negative) co-ions will be repelled from the membrane's anode side to maintain electroneutrality, leading to a drop in electrolyte concentration (C_1 in Figure 8). On the membrane's cathode side, (negative) co-ions are attracted to neutralize the excess (positive) counter-ions transported their through the membrane, leading to enrichment of the electrolyte concentration (C_2 in Figure 8). Equilibrium is reached when the ion drift fluxes is equal to the diffusion fluxes on both sides of the membrane. δ is the diffusion layer distance, and is dependent on the bulk electrolyte concentration, applied field strength, and convection velocity.

Under higher applied electric fields, classical concentration polarization theory must be modified by considering both fluid flow and concentration development to accurately predict experimental results. (33) Solving standard drift-diffusion equation under the condition of strong concentration polarization was shown to lead to a mathematical solution that predicts a space charge region, but it is also important to analyze fluid flow of the system (in addition to diffusion and drift) in order to properly understand the system. In fact, it was theoretically predicted and experimentally shown that a strong, convective flow would exist near the perm-selective nanochannel, which then destroys the concentration gradient (depletion). (34) Due to the coupled nature of this problem, correct modeling of this phenomenon is still challenging and requires substantial scientific studies. The exact fluidic properties and behavior of the ion depletion region are not entirely understood and out of the scope of this thesis. Interested readers are referred to much more detailed discussions in (33).

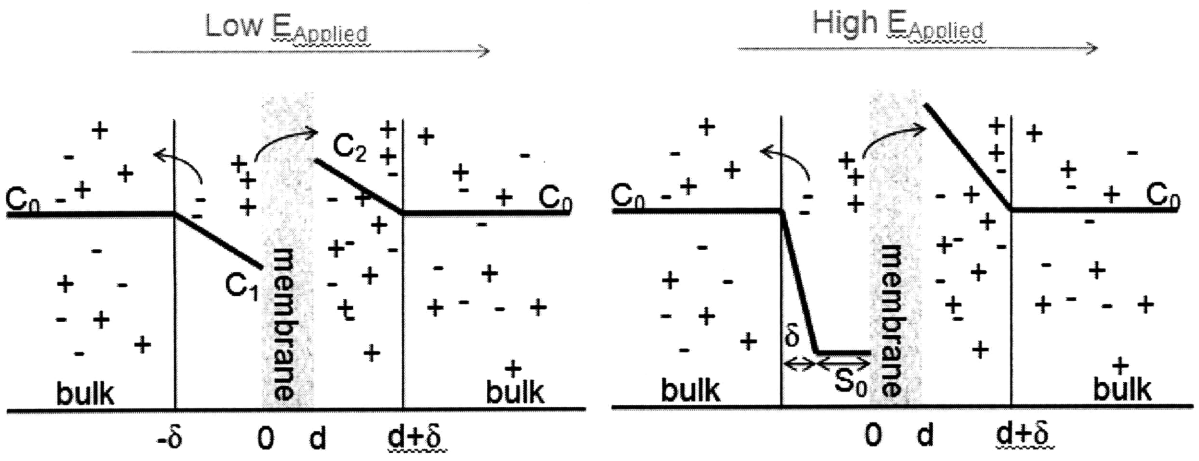

Figure 8: Left: Electrolyte concentration profiles near a charged selective membrane as predicted by classical concentration polarization theory. Right: A large applied electric field induces nonequilibrium convective flow and concentration gradient due to charge selective transport across the membrane.

The mechanism for preconcentration is conceptualized in Figure 9 in a microfluidic format. As drawn in the figure, the device consists of a 20-100μm microchannel connected to other microchannels (not shown) via charge selective membranes. When an electric field is applied through the membrane, counter-ions are removed preferentially from the microchannel through the membrane, and co-ions are repulsed from the region to maintain electroneutrality. An induced ion depletion layer forms outside of the membrane and expands to span the microchannel. This forms a region largely depleted of ions named the depletion zone. Electroosmotic or pressure driven flow is then used to bring in additional charged species, which largely do not cross into the depletion zone and therefore stack up and concentrate at the depletion zone boundary.

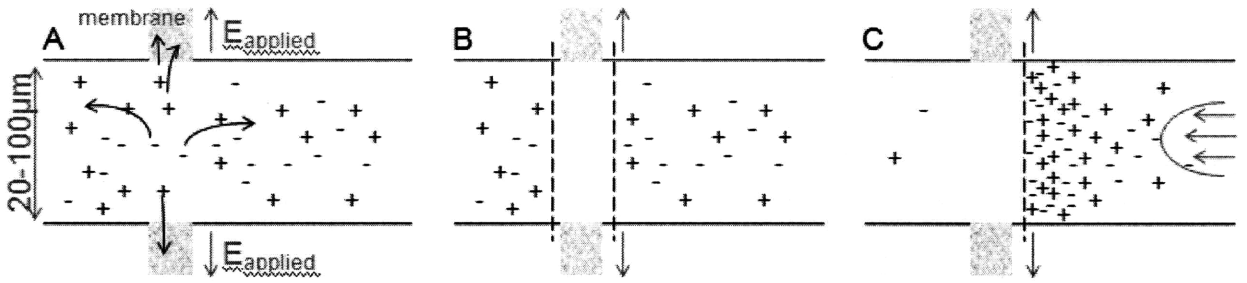

Figure 9: Mechanism of electrokinetic trap development and preconcentration in microfluidic device. A: Applied electric field leads to preferential transport of counter ions through the membrane and repulsion of co-ions to maintain electroneutrality. B: Induced space charge layer (depletion zone) largely free of ions. C: Additional charged molecules brought in by fluid flow stack and concentrate at the depletion zone boundary.

Several micro/nanofluidic device designs take advantage of this preconcentration mechanism by induced space charge layer generation. Wang et.al micromachined a silicon/oxide preconcentration device capable of up to a million times increase in concentration in 1mM phosphate buffer at pH9 in less than one hour of operation. (35) (28)

Lee et. al. created a polydimethylsiloxane (PDMS) device using a micro-patterned charge selective polymer as the charge selective membrane.(36) As shown in Figure 11, the demonstrated preconcentration factor was up to 10^4 in 5 minutes for β- Phycoerythrin protein in 10mM pH7 sodium phosphate buffer. The preconcentration performance was similar to the silicon/oxide design with much simpler fabrication steps, but repeatability suffered somewhat due to the less precise membrane micropatterning process.

Despite very impressive preconcentration performance, the primary of drawback of both designs is electrokinetic instability when operating in higher ionic strength buffers such as cell culture media or blood serum. The instability often prevents the formation of a stable depletion zone. In this thesis, an immunoassay device is presented based on an improvement of the PDMS design capable of operating in cell culture media.

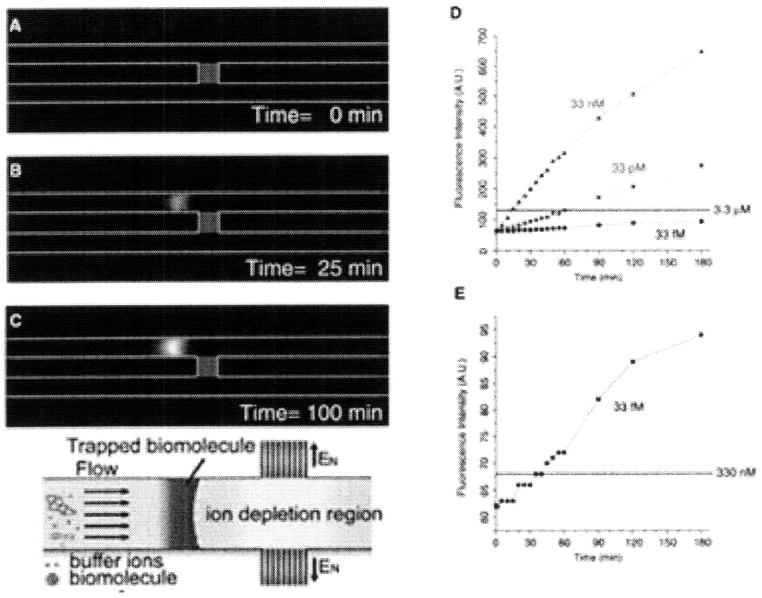

Figure adapted from (35) (28)

Figure 10: Performance and schematic of silicon/oxdie micromachined device. The charge selective membrane is created by reactive ion etching at array of 40nm nanochannels. A/B/C: Fluorescent images taken during the preconcentration of 33fM green fluorescent protein (GFP) in 10mM phosphate buffer. D/E: Fluorescent intensity increase in the concentration zone during preconcentration of GFP at various starting concentrations. Up to 10^6 fold concentration increase can be achieved.

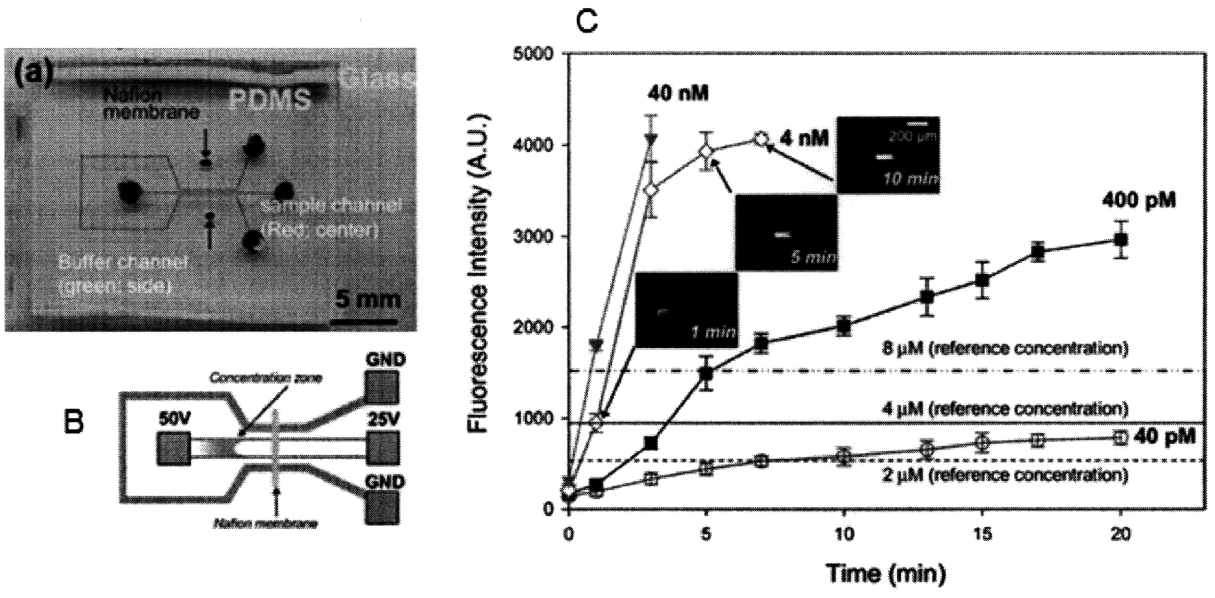

Figure adapted from (36)

Figure 11: Microfluidic preconcentration device fabricated in PDMS with micro-patterned Nafion® polymer as a cation selective membrane. A: Image of the device. B: Operating schematic. C: Preconcentration of β-Phycoerythrin protein in 10mM pH7 sodium phosphate buffer versus electrokinetic trapping time.

Chapter 3: Preconcentration and Immunoassay by Polymer Soft Lithography

Application to Microfluidic Cell Culture Assay and Benefits over Existing Techniques

In this thesis, a novel immunoassay device is presented consisting of integrating a PDMS preconcentrator design with a bead based immunoassay. The integrated immunoassay device can solve the low sample volume problem through direct on-chip coupling to microfluidic cell cultures. Figure 12 diagrams the device's operation principle. PDMS pillar structures are fabricated near the charge selective membrane and used to immobilize antibody functionalized microbeads. Under electrokinetic operation, the concentration zone develops near the microbeads, where the charged antigen molecules collect increase in concentration. When operating with N2B27 cell media, a 200 fold

increase in antigen concentration can be achieved in 30 minutes. The higher antigen concentration near the beads facilitates binding and results in a more sensitive immunoassay.

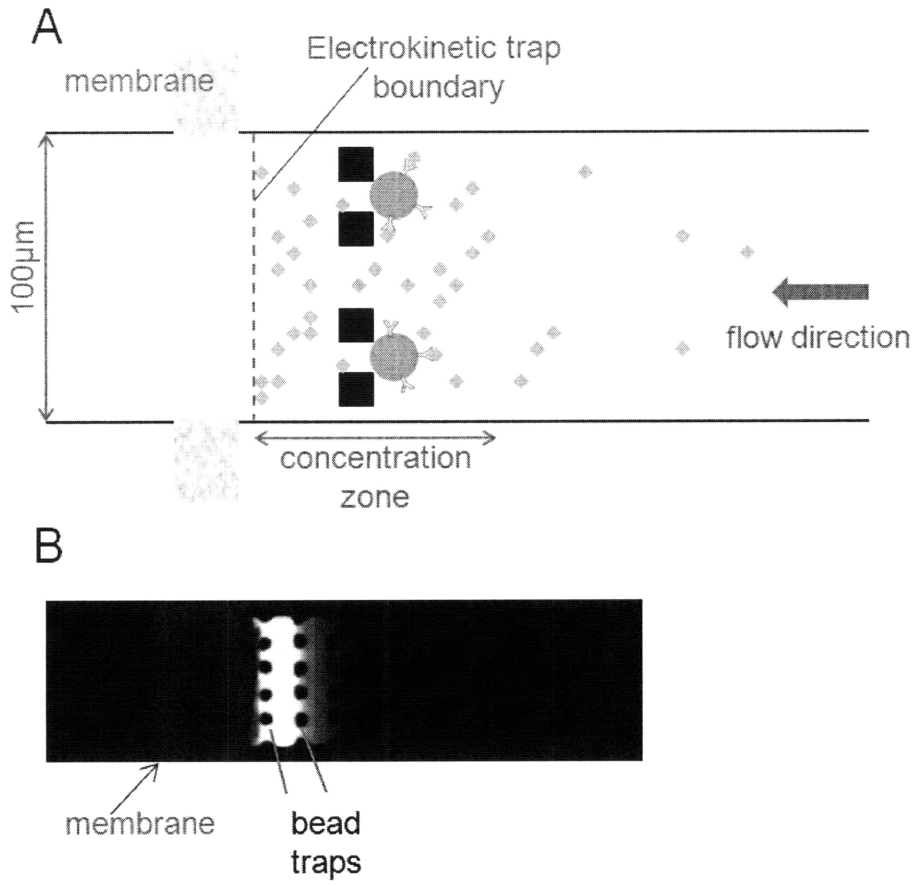

Figure 12: A) Diagram of electrokinetically preconcentrated immunoassay. The conduction of ions through the charge selective membrane leads to formation of the electrokinetic trap. Charged antigen molecules (diamonds) brought in through fluid flow cannot flow past the trap boundary. The increased antigen concentration in this concentration zone favors increased antigen-antibody binding. B) Fluorescent image of R-Phycoerythrin the concentration zone.

The bead based immunoassay device design decouples the microfluidic device design from the antibody immobilization chemistry. The functional attachment of antibodies to microbeads is a well defined, reliable commercial process which occurs outside of the device. When combined with electrokinetic preconcentration, the device enables highly sensitive, multiplexed, and microliter volume antigen concentration measurement which may be performed in near real time requiring only the replacement of beads. Unlike sensor miniaturization or novel transduction strategies which require complicated

clean room fabrication or delicate electronics, the device requires only a single lithography mask with 5μm resolution and can be operated with a simple fluorescent microscope.

Device Design and Fabrication

Microchannel Fabrication

Fabrication for the device is divided into two processes. The first occurs in the clean room to create a silicon master for the device microchannels, and the second is the polymer patterning process which can be performed outside of the clean room. We fabricate the PDMS structure containing microchannels by soft polymer lithography. (Figure 13). First, we create a photomask by printing the microchannel design onto a glass plate (Fineline Imaging, Colorado Springs, CO). Contact lithography (EV1, Electronic Vision Systems, AZ) with this mask was used to pattern thin photoresist (~1μm height) on a 6in silicon wafer, followed by deep reactive ion etching (DRIE, Surface Technology Systems, United Kingdom) using SF_6 etchant and C_4F_8 passivation (Bosch process) to a depth of 10 microns. The relatively large 5μm feature size and uniform 10μm required etch depth leads to a relatively simple fabrication process, as only a single mask is needed and the DRIE to 10μm is easily achieved without complicated recipes. After stripping the photoresist using oxygen plasma, a perfluorinated trichlorosilane (T2492-kg, United Chemical Technologies, Bristol, PA) is evaporated next to the silicon master inside a vaccum chamber to deposit silane onto the wafer and cover the exposed silicon surface. We then mix PDMS prepolymer and curing agent (Dow Corning Sylgard 184 Silicone Elastomer Kit) in a 10:1 ratio. After degassing in a vacuum chamber, we pour the PDMS liquid mixture onto the silicon master and cure the polymer at 120°C for 15 minutes. The cured PDMS does not bond to the silane coated surface and can be peeled off the mold and cut to individual dies. We then drill 1mm diameter holes vertically into the PDMS to create the fluid connections to the microchannels.

1.Blank silicon wafer	2.Coat photoresist	3.Expose through photomask
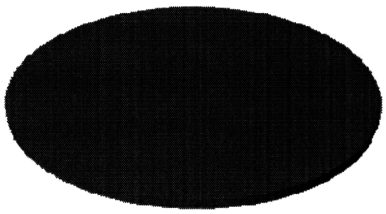	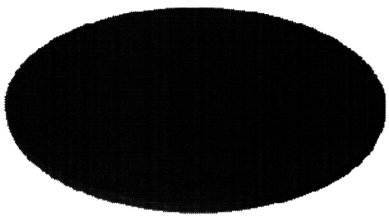	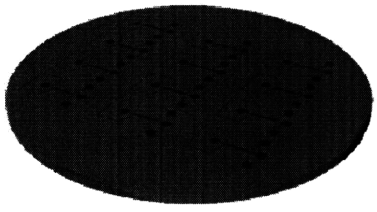

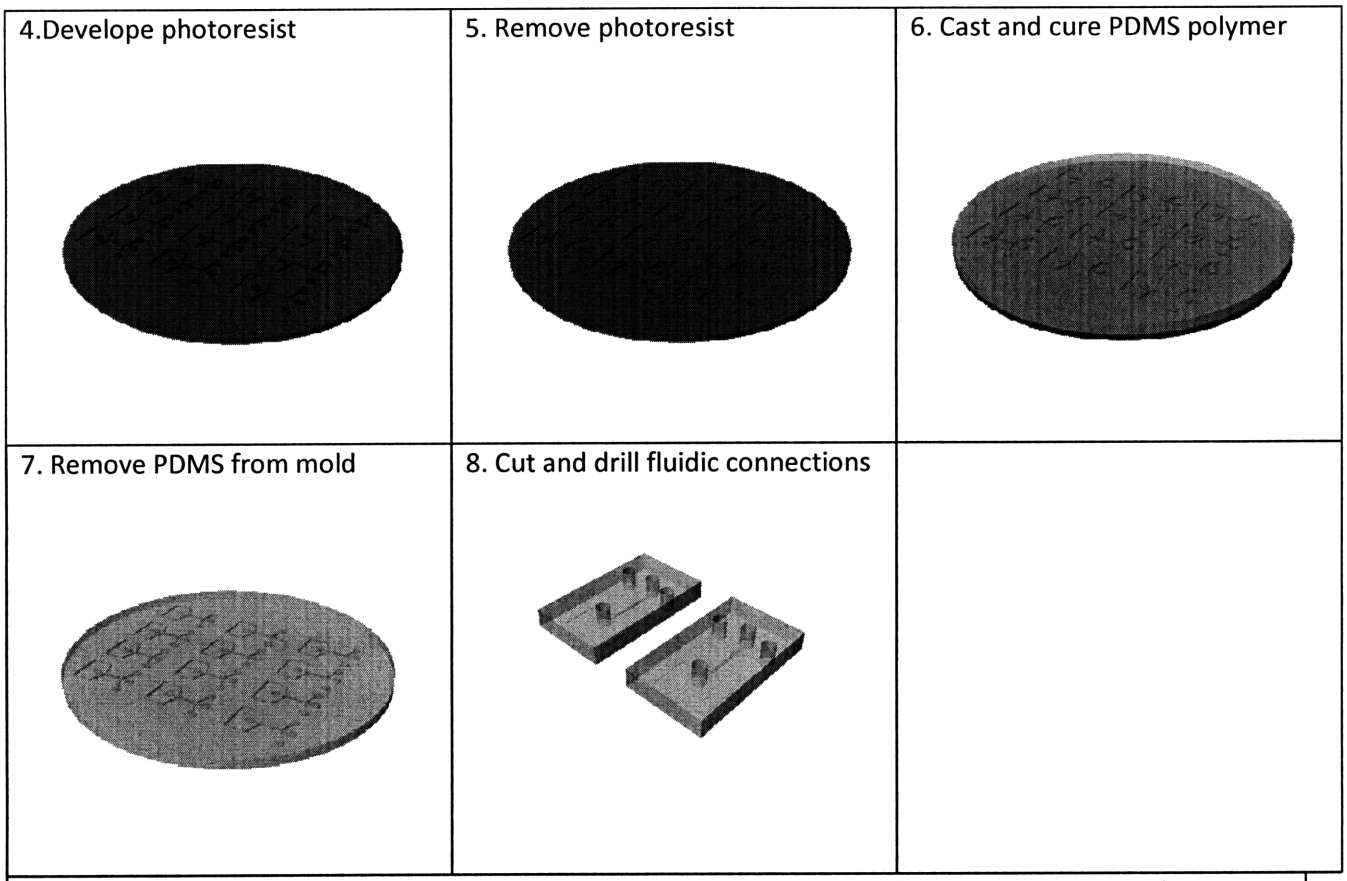

Figure 13: Device microchannel fabrication steps. 1. Silicon wafer. 2. spin coat photoresist to a height of 1μm. 3. Expose to UV with photomask to define microchannel pattern. Photoresist not covered with mask features become soluble to the developer. 4. Deep reactive ion etching with SF_6/C_4F_8 Bosch process etches silicon from the wafer in areas not protected by photoresist to 10μm. 5. Plasma ashing with oxygen gas to remove photoresist. The result is a mold of the microchannel features in monolithic silicon.

We then create the nanochannel structures needed to bridge the device's main and side channels, as shown in Figure 14. Clean glass microscope slides are baked at 200°C for approximately 15 minutes for dehydration and to ensure a hydrophilic surface. A PDMS chip containing a single 1cm long, 100μm wide, and 50μm high microchannel is reversibly bonded to the glass slide. We place a small drop of Nafion® perfluorinated resin solution (product number 527122, Sigma-Aldrich, St Louis, MO) in one reservoir and apply negative pressure at the other reservoir. When the channel is filled with the resin solution, we peel off the PDMS and place the glass slide on a 95°C hotplate for approximately 10 minutes to cure the resin. Finally, the PDMS microchannels and glass slide is treated with oxygen plasma and irreversibly bonded. Alignment of the microchannel features and Nafion® resin pattern is performed using a stereomicroscope. The flexible PDMS is capable of sealing around the cured resin

without visible fluid leakage during the experiment. Since the Nafion® resin contains 80% solvent, the height of the membrane is much less than the channel depth. Therefore, fluid flow through the channels is not impeded by the membrane. The finished device is then baked on a 95°C hotplate overnight to improve bonding, and then stored under vacuum. Vacuum storage removes air from PDMS and minimizes the appearance of air bubbles when the device is used.

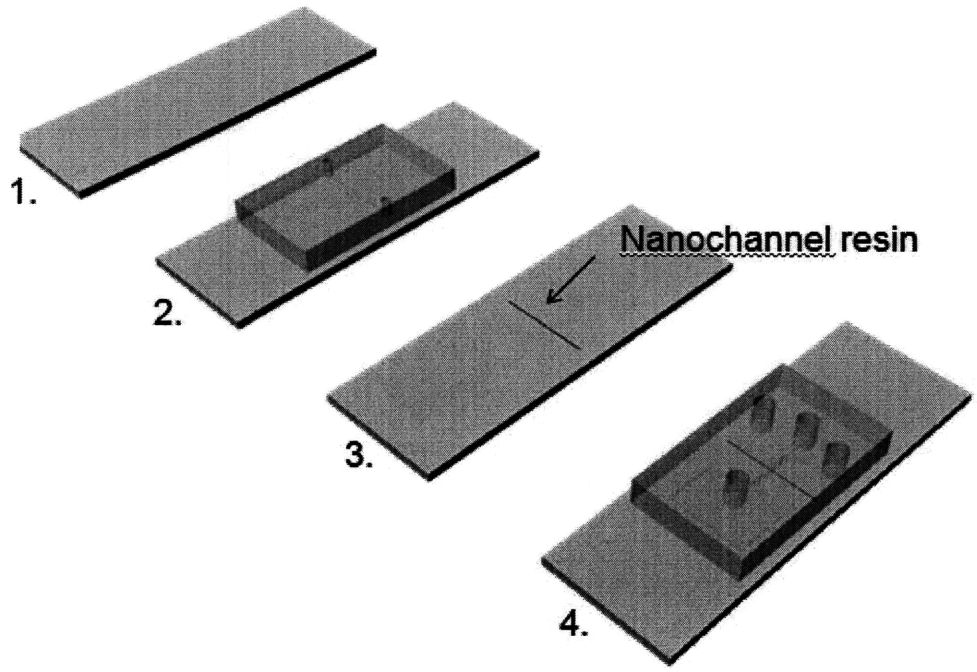

Figure 14: Device nanochannel patterning bonding. 1. Plain microscope slide. 2. Reversible bonding of PDMS chip with patterning channel. The patterning channel is filled with Nafion® prepolymer. 3. The PDMS patterning chip is removed, and the Nafion resin solidifies following 95°C bake for 5 minutes. 4. The PDMS chip containing the device microchannels and glass slide is exposed to oxygen plasma and irreversibly bonded.

A top down schematic and bright field image of the device is shown in Figure 15. The device consists of a main channel (reservoirs V_c and V_m) surrounded by a side channel (reservoirs V_s). The mechanism of operation will be described in a later section.

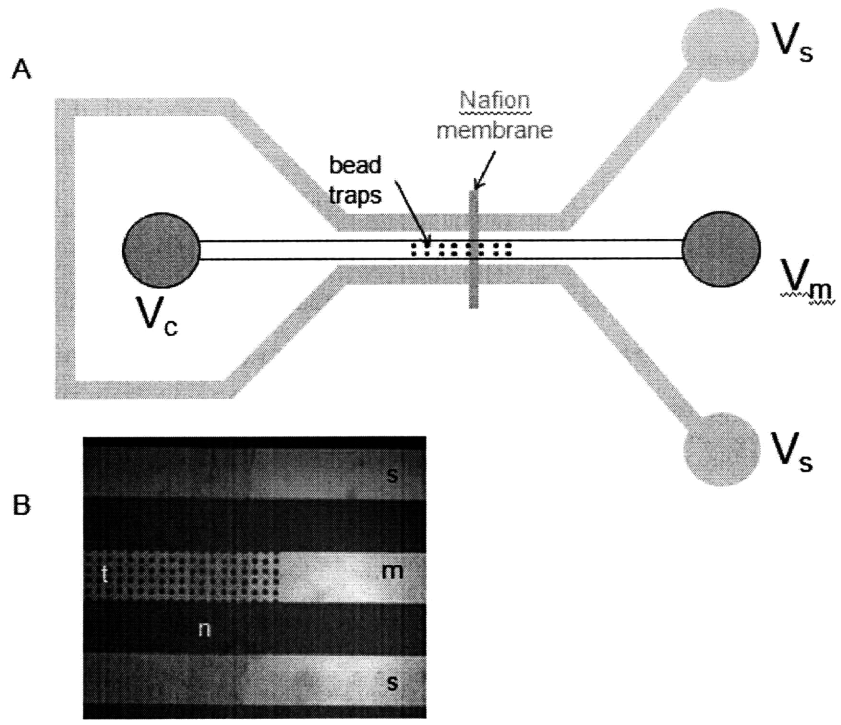

Figure 15: Top down schematic of the immunoassay device. A: The device consists of one main channel (reservoirs V_c and V_m) and one side channel (reservoirs V_s). The two channels are connected near the bead traps by the Nafion® charge selective membrane. B: Bright field image of the device near the Nafion® membrane. m: main channel, s: side channel, t: bead trap features, n: Nafion® membrane. The height of the membrane is significantly less than the channel depth and does not impede fluid flow.

Bead Functionalization and Immobilization

FMAT® streptavidin functionalized 6-8μm polystyrene beads (0.5%w/v, Applied Biosystems) were used as solid support for the device's capture antibodies. A mixture of 320μL of beads, 800μL of 1X PBS at pH 7.4, and 2μg of biotin conjugated anti-R-Phycoerythrin (RPe) were incubated in a centrifuge tube for 8 hours. The mixture is then centrifuged to remove the supernatant several times followed by resuspension of the beads in 1X PBS with 1% bovine serum albumin (BSA). Removing the supernatant washes away excess unbound antibodies and the BSA reduces nonspecific binding inside the mixture.

This process of bead functionalization is a well established commercial process and very repeatable so long as there is an excess of antibody to streptavidin binding sites. Functionalization processes which happen outside of the microdevice are preferable since they decouple the device design from the need to consider complicated surface chemistries which often need to be tailored to each antibody or other

molecule. We have chosen to attach antibodies for our immunoassay device, but other biomolecules such as enzymes and DNA probes may be similarly attached by the same streptavidin-biotin interaction and used in our device without modification. Furthermore, the use of beads as mobile solid supports allows us to control the movement of functionalized antibodies in the device. The enables longitudinal immunoassay studies in the same device simply by replacing the beads when needed.

Bead immobilization is shown in Figure 16. This process is adapted from the technique developed by Di Carlo et. al. (37) The bead traps are PDMS features in the main channel. When a bead trap is empty, the fluidic resistance through the trap is approximately equal to the resistance of the flow paths around the trap. When a bead fills and blocks the trap, the fluidic resistance becomes much larger and the resulting fluid flow diverts other beads to other traps further downstream. This immobilization method mostly leads to one immobilized bead per trap with fairly good repeatable results. Furthermore, the simple pillar features needed to fabricate the traps are uniform in height with the channel wall, thus allowing single mask fabrication. The main drawbacks are in difficulties removing the bead from the device once trapped and the constant need to maintain the pressure gradient to keep the beads from diffusing away.

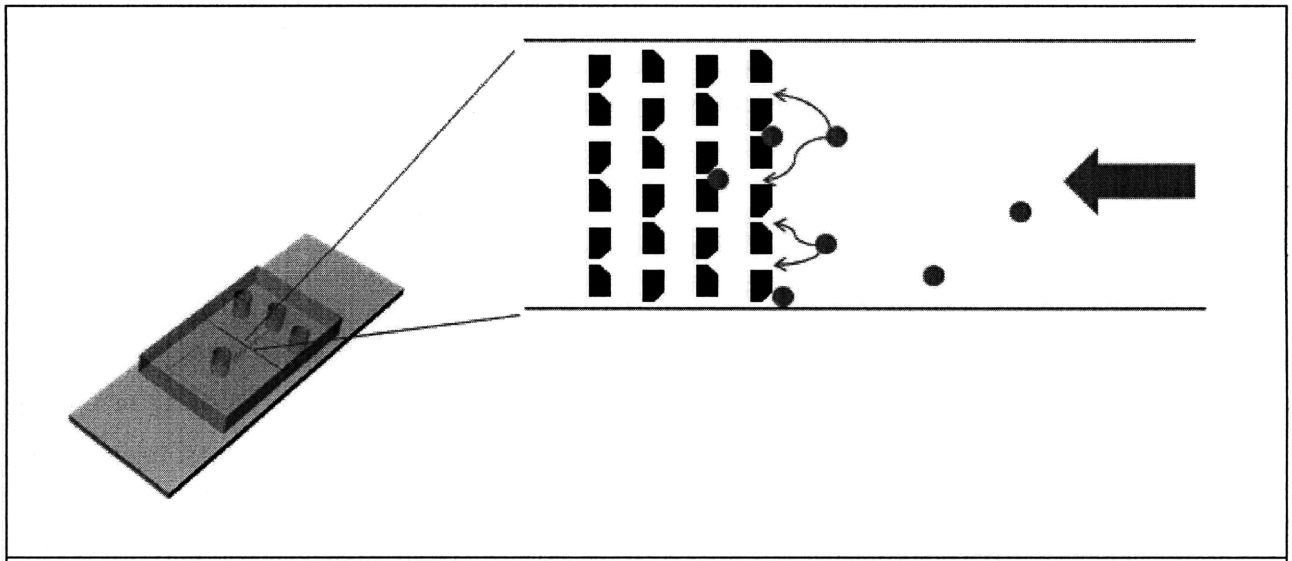

Figure 16: Immobilization of antibody-labeled microbeads in the main channel adapted from (37). The technique's main principle is fluidic resistance modulation. When a bead fills the trap, the fluid path through the trap is blocked and subsequent beads flowing in are directed towards other traps downstream.

Immunoassay without Preconcentration

Baseline immunoassay results were obtained using the device without preconcentration. Following immobilization of anti-RPe functionalized beads in the main channel, a syringe pump was used to incubate the beads in N2B27 stem cell media with various concentrations of RPe added. The fluorescent RPe molecule causes the anti-RPe functionalized beads to fluoresce when captured by the antibody.

Fluorescent imaging was performed using an inverted epi-fluorescence microscope (IX-71, Olympus, Melville, NY) with a thermoelectrically cooled CCD camera (Sensicam QE, Cooke Co., Auburn Hills, MI) and a 100W mercury lamp (Chu Technical Corp., Kings Park, NY). The RPe fluorescence was visualized using a TRITC filter set (excitation 562nm, emission 624nm, Semrock, Rochester, NY). Exposure time was precisely controlled through a programmable mechanical shutter to minimize sample photobleaching. Images were analyzed using the IPLab imaging processing software (IPLab 3.5, Scanalytics, BD Bioscience, Rockville, MD).

Immunoassay results for the detection of RPe without preconcentration is shown in Figure 7. Equilibrium antigen-antibody binding have been reached for incubation with RPe concentrations above 1μg/ml (>1mm/s), where the intensity versus time curve approaches the equilibrium value exponentially. At lower concentrations, the binding response becomes roughly linear, and the equilibrium value is not reached within the one hour experiment. Figure 7B compares the 30 minute incubation result to the 60 minute experiment. Despite doubling the incubation time, the detected intensity only increased marginally, suggesting that increasing the incubation time is an inadequate way to improve immunoassay performance.

Immunoassay with Preconcentration

The operating parameters for preconcentration are shown in Figure 17. Pipette tips are inserted into the fluid connections of the device and act as fluidic reservoirs. The outer side channel is filled with 1X PBS, with pressure balanced at the reservoirs V_s by filling the pipette tips to an equal level. The main channel reservoirs are filled with the sample under detection and the reservoir relative levels (channel pressure) are optimized for stability and speed of preconcentration. We used 1X PBS (P3813, Sigma-Aldrich, St Louis, MO, NaCl 0.138 M; KCl 0.0027 M) or N2B27 media with 1μg/ml green fluorescent protein (GFP, ~28kDa, pI=6) and the varying concentrations of R-Phycoerythrin (RPe, ~270kDa, pI=4.5). GFP is used as a fluorescent tracer to allow us to set the correct flow conditions and voltages for each

experiment, and RPe is the protein under detection and targeted by the capture antibodies. Control experiment were performed to no cross reactivity between anti-RPe and GFP.

The applied electric field across the Nafion® membrane is set by modulating the voltages at the V_s and V_m reservoirs. The voltages are set by placing platinum wires into the reservoirs and connecting them to a power supply. Generally, V_s is grounded and V_m is dynamically changed to optimize for stable depletion and concentration zones. Both the main channel pressure and V_m voltage are strongly dependent on the buffer or media in the main channel. When the proper pressures and voltages are set and depletion zones balanced, electrokinetic preconcentration proceeds, and proteins (and other charged molecules) stack up inside the concentration zone.

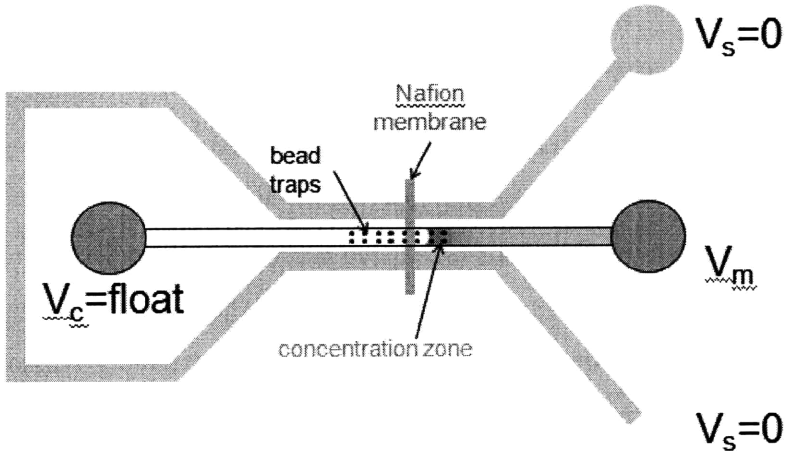

Figure 17: Diagram of preconcentration device operation. The center channel is filled with the sample in cell culture media media or PBS and the side channel is filled with PBS buffer. Positive pressure driven flow is set by controlling the liquid column heights between the V_m and V_s reservoirs. When appropriate voltages are set as indicated and Vm is dynamically determined, electrokinetic preconcentration proceeds and antigen accumulate in the concentration zone.

The preconcentration of 1µg/ml RPe in N2B27 media is shown in Figure 18. The preconcentration factor in this case is approximately 200 over 30 minutes.

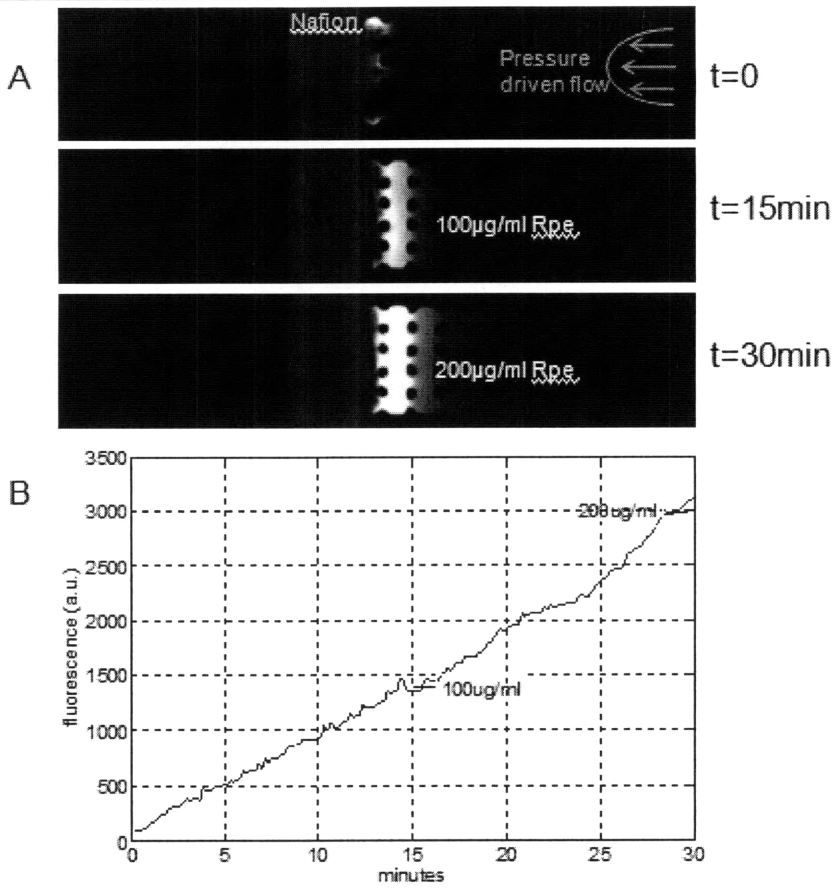

Figure 18: Preconcentration of 1µg/ml RPe in N2B27 media using immunoassay device. A: Fluorescence image of the concentration zone at various times. B: average fluorescence values of the concentration zone versus time. The preconcentration factor is 200 over 30 minutes.

The impact of preconcentration on the RPe concentration distribution is shown in Figure 19, where the preconcentrated immunoassay was performed for 1ng/ml RPe in N2B27 media. The beads in the concentration zone near the Nafion membrane captured the most RPe molecules and had the highest fluorescent intensity. Upstream of the concentration zone, the beads were less flourescent as these beads encountered RPe at the base concentration of 1ng/ml. The downstream beads are extremely faint and almost not visible. This is because only a small amount of RPe escaped downstream from the concentration zone and across the electrokinetic depletion boundary. Figure 20 shows similar results in a comparison of bead intensities upstream, downstream, and at the Nafion membrane over many experiments and at several RPe concentrations.

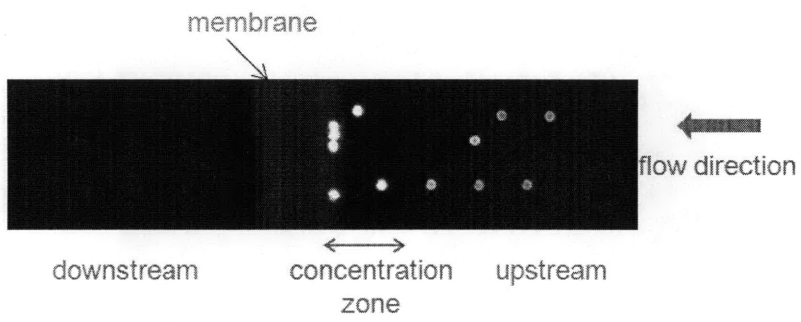

Figure 19: Fluorescent image showing captured RPe molecules on anti-RPe functionalized beads after 30min preconcentration of 1ng/ml RPe in N2B27 media. Due to preconcentration, the intensity of beads in the concentration zones is higher than those in the unconcentrated zone upstream. Only a small amount RPe escapes the concentration zone and flows downstream, as evidenced by the very faint intensity of the downstream beads.

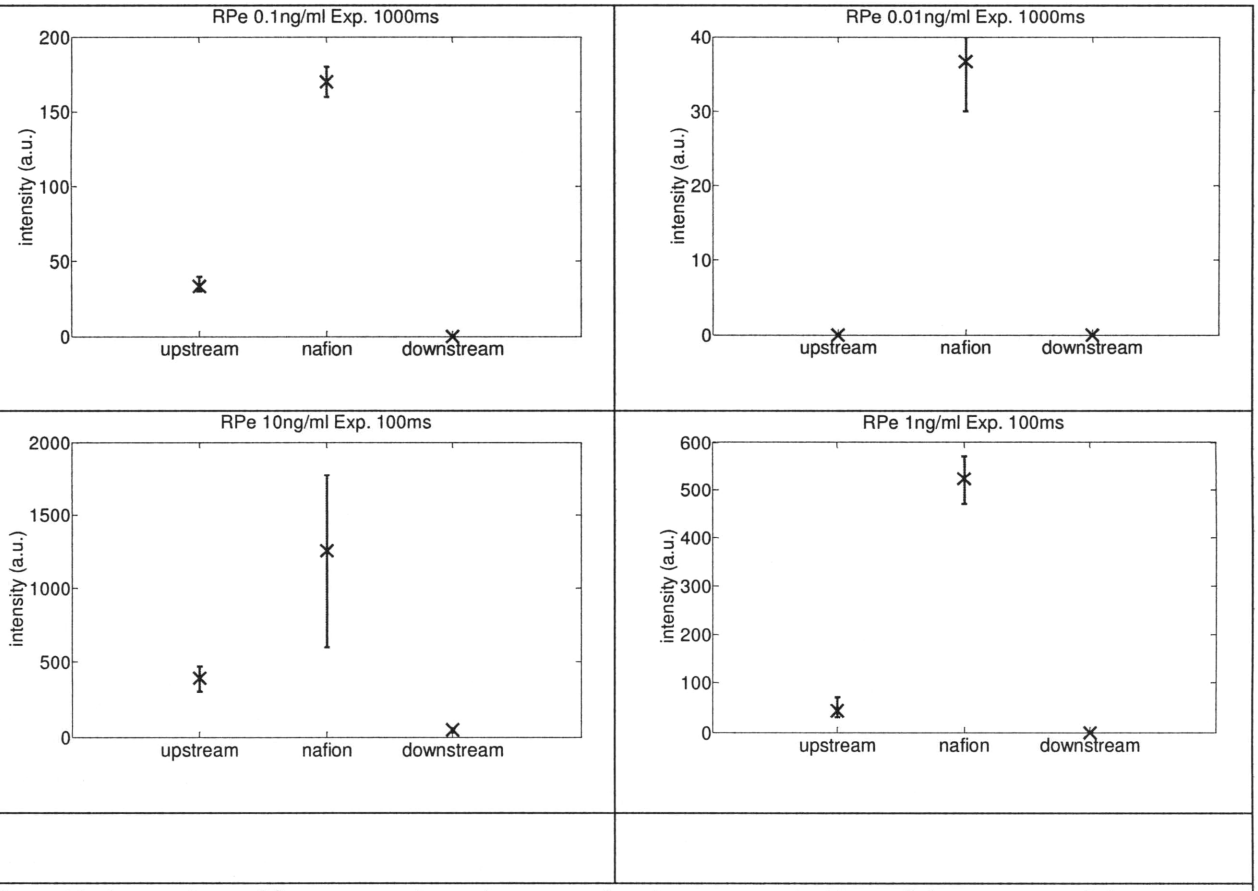

Figure 20: Comparison of fluorescence intensity among beads upstream, inside, and downstream of the concentration zone after 30min preconcentrated immunoassay of RPe in N2B27 media.

The results of 30min preconcentrated immunoassays for various concentrations of RPe in N2B27 media are compared to the incubation only immunoassays in Figure 21. At each concentration of RPe, the preconcentrated immunoassay resulted in higher antibody-antigen binding, as evidenced by the increased fluorescent intensity from captured RPe on the microbeads. The sensitivity for RPe without preconcentration using our experimental setup is 1ng/ml while consuming 30-60µl of sample. Preconcentration improved the detection sensitivity by 100 fold to 10pg/ml. The sample consumed during preconcentration was measured to be less than 1µl based on measuring the level of sample remaining in the inlet reservoir.

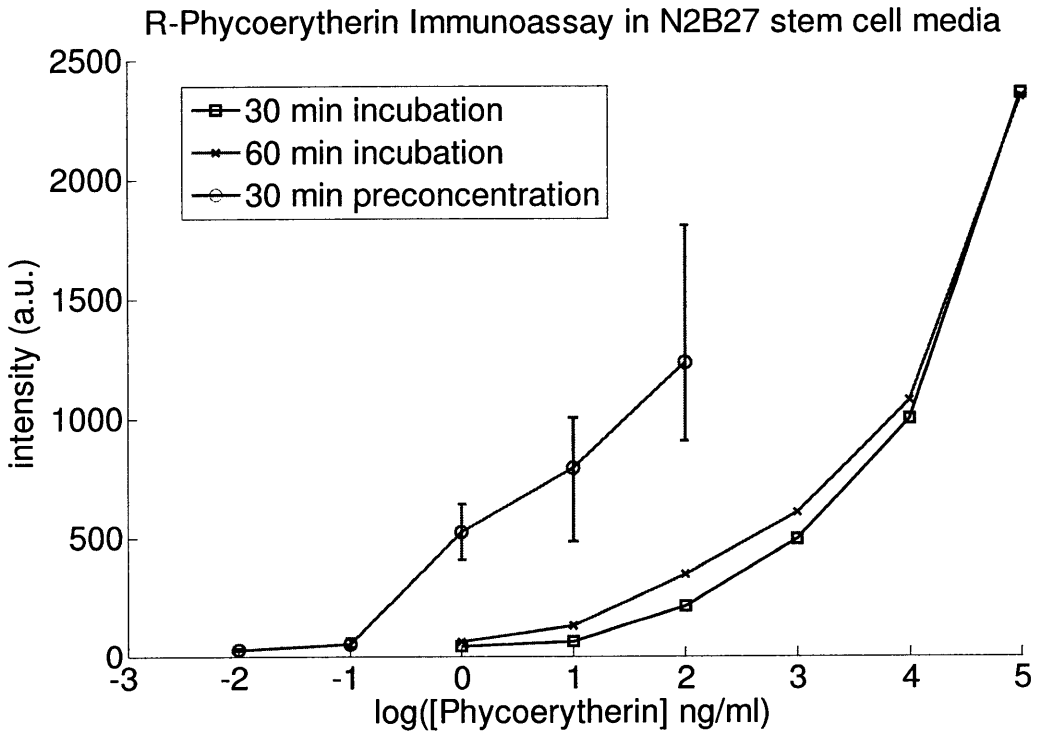

Figure 21: Immunoassay to detect RPe in N2B27 media with 30 minute preconcentration. Preconcentration improved detection performance by approximately 2 orders of magnitude. All assays were performed using the same optics setup and exposure settings.

In Figure 22, the function of the preconcentrated immunoassay device was extended to detect the non-fluorescent antigen C-Reactive Protein (CRP). Preconcentration of CRP in N2B27 stem cell media was

performed near anti-CRP functionalized beads, followed by flowing in 10μg/ml FITC-anti-CRP as a detection antibody. Both the incubation and preconcentration curve was obtained using a flow rate of less than 1μL a minute, to approximate the amount of sample available for microfluidic cell cultures. The demonstrated signal enhancement was 10 fold.

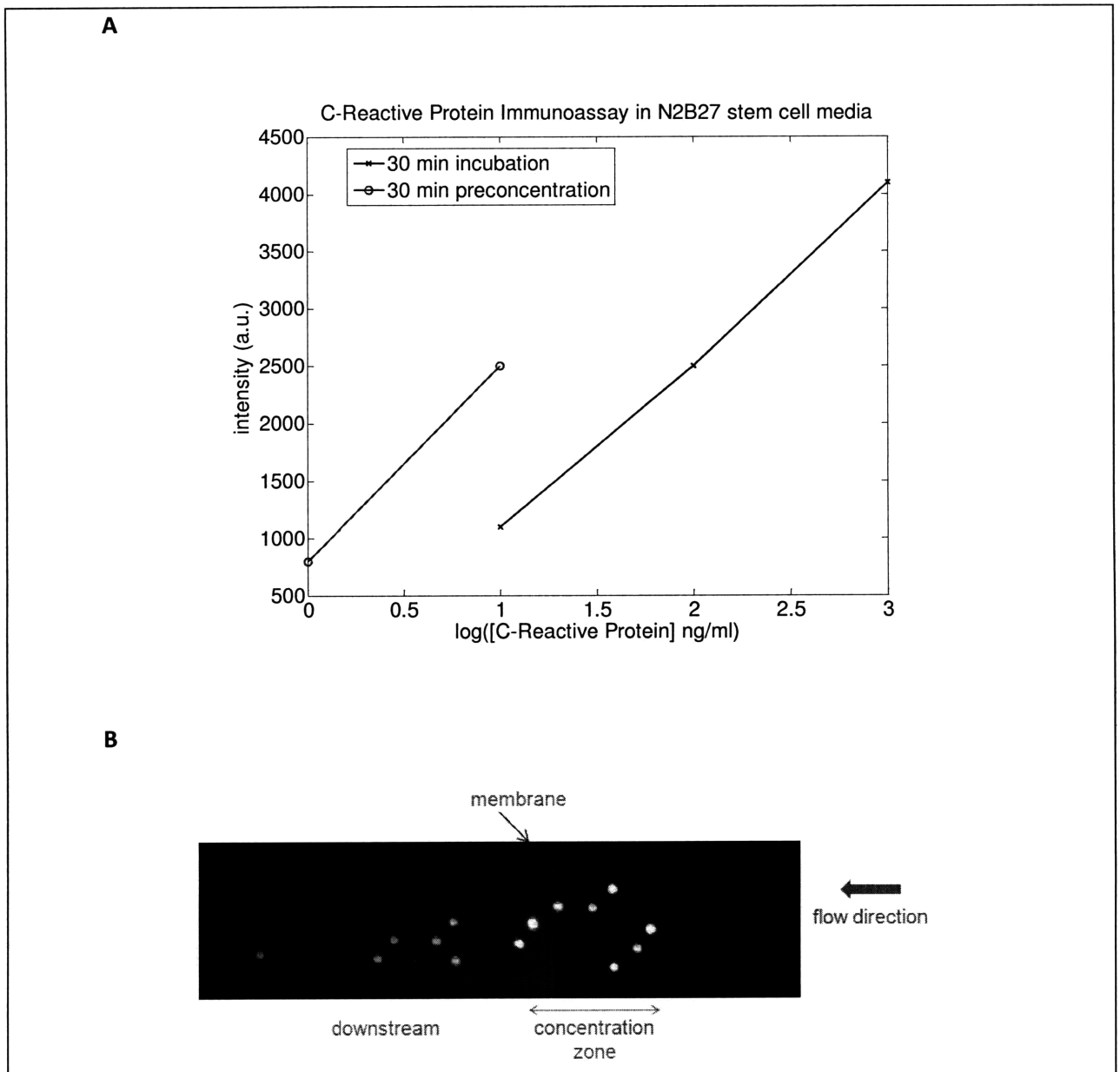

Figure 22: A. Immunoassay to detect RPe in N2B27 media with 30 minute preconcentration. B. Fluorescence of FITC-anti-CRP after 1ng/ml CRP preconcentrated assay. The higher concentration of CRP in the preconcentration zone (right of Nafion) results in greater capture of CRP and higher fluorescence.

Discussion and Significance of Results

The novel PDMS microfluidic immunoassay device described in this thesis is the first to successfully demonstrated detection of a nonfluorescent protein antigen directly from cell culture media. We have demonstrated an a reduction in the detection limit of RPe by two orders of magnitude and demonstrated the improved detection of CRP by sandwich immunoassay based on the principle of electrokinetic pre-binding amplification. Importantly, the detection was conducted directly from N2B27 cell culture media and consumed less than 1μL of sample. The use of prebinding amplification to achieve higher immunoassay sensitivity while consuming lower amounts of sample potentially allows the preconcentrated immunoassay device to achieve direct detection of low abundance antigens from microfluidic cell cultures. Furthermore, since electrokinetic preconcentration is used to improve binding dynamics before use of the secondary antibody, the device can be engineered readily to include postbinding amplification to achieve higher sensing performance.

Electrical Profile Measurement near the Charge Selective Membrane

Electrokinetic trapping's principle of operation is based on the depletion and enrichment effects which accompany charge selective transport. Since the ion concentration near the charge selective membrane is depleted, the potential drop across the entire microchannel becomes focused on the depletion zone. Furthermore, the lower ionic strength results in an effectively lower zeta potential. These two effects combine to create an amplified electrokinetic response characterized by fast following rotating vortices. (38)The electrical field distribution which drives this electrokinetic response, however, has never been measured. In this section, we describe the results of electrical field measurements conducted near the Nafion membrane in a PDMS preconcentration device.

Figure 23 shows the microfluidic preconcentrator design used for the electrical measurements, where integrated microelectrodes are fabricated on the glass cover of the device to provide electrical access to the microchannels. The fabrication of the electrodes proceeds as follows. First, standard photolithography is used to pattern NR7 photoresist to a thickness of 3μm onto a pyrex wafer. We then expose the wafer to UV through a mask rendering the electrode pattern soluble to the developer. Following development, a layer of 10nm titanium followed 90nm of gold is deposited over the wafer using electron beam deposition (Temescal Semiconductor Products). The wafer is then incubated in acetone to dissolve all exposed photoresist areas and lifts off the deposited metals except at the electrode pattern. The wafer is then diesawed and fabrication then proceeds with membrane

patterning and bonding to the PDMS microchannels structure as described in the previous chapter. The PDMS microchannels structure is bonded with the microelectrodes open to the main microchannel near the Nafion membrane. The PDMS structure covers only half of length of the electrodes, allowing wires to be soldered onto the exposed portion.

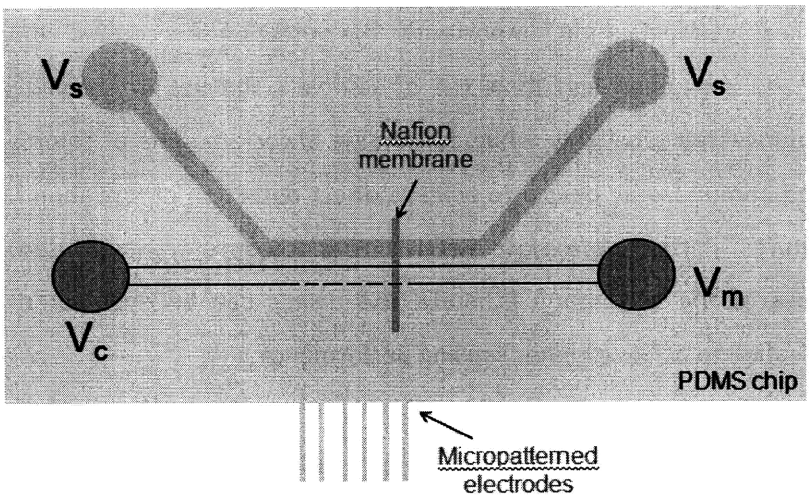

Figure 23: PDMS preconcentrator with integrated electrodes for electric field measurement near the charge selective membrane.

During device operation, all the pressures at the four reservoirs are balanced. All channels are filled with 10mM sodium phosphate buffer at pH 9 and 10nM fluorescein isothiocyanate (FITC). Electrical input to the preconcentrator is provided by inserting platinum wires into the reservoirs. The reservoirs at V_s are electrically grounded and the voltages at V_m and V_c are chosen dynamically to stabilize the concentration and depletion zones. This scheme is slightly different from the one used in the immunoassay, which utilizes a pressure driven flow to establish the concentration zone. The voltages between microelectrodes are sampled using a Keithley 236 current/voltage source-measure unit (Keithley Instruments, Inc.) whose high input impedance (200TΩ) will ensure minimal interference with the depletion and concentration processes. The size and profile of the concentration and depletion zones near the membrane is indicated by the brightness of the FITC dye. We then correlate these profiles to the electrical profile measured on the microelectrodes to study the preconcentrator's electrokinetic behavior.

A typical time response of the electric field strength after voltage is applied is shown in Figure 24, where the operating voltages are V_c=50V, V_m=20V, and Vs=0V. In the device measured, the Nafion membrane is patterned between the v_5 and v_6 electrodes. During preconcentration, the depletion region partially covers the region between v_3 and v_4 and the entire region near v_4 and v_5. As preconcentration starts, the charge selective transport of ions through the membrane leads to an amplified electric field in the lower ionic strength depletion region. The depletion region is then seen expanding away from the membrane, corresponding to the increase in electric field strength between v_3 and v_4. For the most part, v_{12} and v_{23} remains constant near 60V/cm. This is because the depletion and concentration zones do not include the space between v_1 and v_3 for the duration of the experiment. There was nearly linear voltage drop from the reservoir to the concentration zone, a distance of 0.5cm (30V/0.5cm=60V/cm). These results are in compliance with recent one-dimensional modeling studies. (39,40) The potential drop from v_5 to v_6 is initially negative and gradually increases. A nonzero voltage voltage between v_5 and v_6 is seen even when the operation voltage is not set. This is because the channels are flushed with electroosmotic flow which interacts with the Nafion membrane to generate depletion and enrichment effects even without electrically connecting the side channels. The measurement results across multiple experiments tend to create variable profiles of v_{56} depending on the initial statement from electroosmosis as well as the charge profile of the side channel and membrane. The presence of a negative voltage drop from v_5 to v_6 is seen stably across many experiments and indicates the direction the electroosmotic flow in the device is towards the membrane from both sides of the channel. The flow direction however, is left to right due to the much greater amplified electrokinetic response in the depletion zone.

These integrated microfluidic electrodes are the first time direct, spatially resolved voltage measurements are made for microfluidic electrokinetic preconcentration and provides an electrical profile for the study of electrokinetic preconcentration behavior. From the practical standpoint, correlation of this electrical profile to the location of the depletion region may allow us to track the concentration zone and set the electrical and pressure operating parameters without the need for a fluorescent tracer.

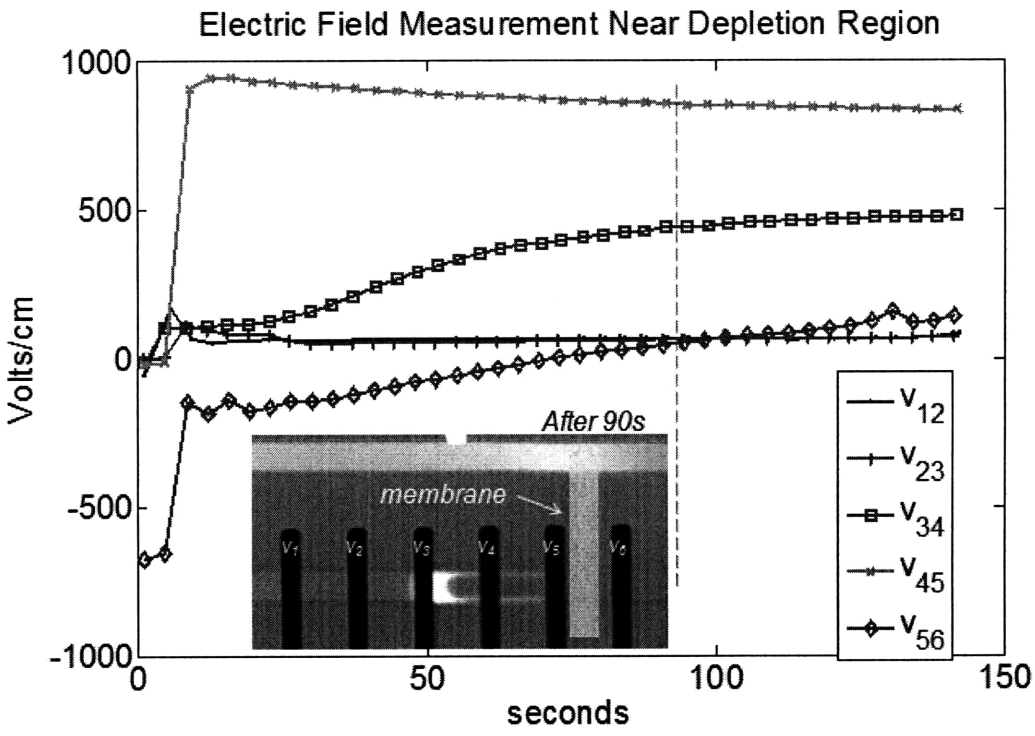

Figure 24: Electric field strength near the Nafion membrane as measured by integrated microelectrodes. The lower ionic strength in the depletion region results in an amplified electric field.

Future Work

Continued development of the preconcentrated immunoassay may be directed towards integration with novel microfluidic cell culture experiments. As microfluidic cell cultures can better mimic *in vivo* microenvironments through precise control of perfusion conditions and culture geometry, the integration of the preconcentrated immunoassay with microfluidic cell cultures will lead to an important new tool to study cell biology. Specifically, the next steps in the development of this immunoassay are:

1. Miniaturization of the preconcentrator by one order of magnitude to a main channel cross section of 10μm by 1μm. The electrokinetic trapping effect of the preconcentrator depends on the formation of the ion depletion region in the microchannel, which is an extension of the electrical double layer in the charge selective membrane. The high ionic strength of the cell media decreases the electrical double layer width decreases, thus weakening the SCL. While we have demonstrated the operation of preconcentrated immunoassay in cell media, the device

requires a more stable operation profile to be useful as a quantitative tool. Decreasing the dimensions of the microchannel compensates for the weakening depletion forces.

2. Due to the reduced channel dimensions, an alternative to the bead based solid support may be needed. The most promising is patterning the antibody directly to the glass slide of the device. Several surface chemistries are available, but the most straightforward technique is the use of a patterning channel (similar to the Nafion® membrane patterning channel used currently) to nonspecifically absorb a streptavidin pattern onto the glass slide. Biotin conjugated antibodies can then be spotted onto the streptavidin to bind capture antibodies in the correct capture orientation.

3. Fluorescent tracer characterization. For preconcentrated immunoassays, a fluorescent tracer is needed to dynamically set the correct operating pressures and voltages. Proteins of different pI values and molecular weights are affected by the depletion and trapping forces differently. The choice of a fluorescent tracer needs to be determined carefully for each protein antigen.

4. Integration of device with microfluidic cell culture and perform preconcentrated immunoassay directly from cell secretions. We propose of the use of NIH/3T3 cells and assay for the cytokine IL-6. IL-6 is secreted from 3T3 fibroblasts at a basal rate but increases when simulated with certain signaling peptides. (41). In this study, the time course of IL-6 secretion as a function of stimulation will be tracked.

References

(1) Tini M, Jewell UR, Camenisch G, Chilov D, Gassmann M. Generation and application of chicken egg-yolk antibodies. Comp.Biochem.Physiol.A.Mol.Integr.Physiol. 2002 Mar;131(3):569-574.

(2) Cole SP, Campling BG, Atlaw T, Kozbor D, Roder JC. Human monoclonal antibodies. Mol.Cell.Biochem. 1984 Jun;62(2):109-120.

(3) Nakamura RM. Immunochemical Assays and Biosensor Technology for the 1990s. 1st ed. Washington D.C.: American Society for Microbiology; 1992.

(4) de Jager W, Rijkers GT. Solid-phase and bead-based cytokine immunoassay: A comparison. Methods 2006 4;38(4):294-303.

(5) de Jager W, Prakken BJ, Bijlsma JWJ, Kuis W, Rijkers GT. Improved multiplex immunoassay performance in human plasma and synovial fluid following removal of interfering heterophilic antibodies. Journal of Immunological Methods 2005 5;300(1-2):124-135.

(6) Nair PR, Alam MA. Performance limits of nanobiosensors. Appl. Phys. Lett. 2006 5 June 2006;88(23):233120.

(7) Kusnezow W, Syagailo YV, Ruffer S, Klenin K, Sebald W, Hoheisel JD, et al. Kinetics of antigen binding to antibody microspots: strong limitation by mass transport to the surface. Proteomics 2006 Feb;6(3):794-803.

(8) Hwang KS, Lee JH, Park J, Yoon DS, Park JH, Kim TS. In-situ quantitative analysis of a prostate-specific antigen (PSA) using a nanomechanical PZT cantilever. Lab.Chip 2004 Dec;4(6):547-552.

(9) de Mol NJ, Plomp E, Fischer MJ, Ruijtenbeek R. Kinetic analysis of the mass transport limited interaction between the tyrosine kinase lck SH2 domain and a phosphorylated peptide studied by a new cuvette-based surface plasmon resonance instrument. Anal.Biochem. 2000 Mar 1;279(1):61-70.

(10) Pampaloni F, Reynaud EG, Stelzer EH. The third dimension bridges the gap between cell culture and live tissue. Nat.Rev.Mol.Cell Biol. 2007 Oct;8(10):839-845.

(11) Ghosh S, Spagnoli GC, Martin I, Ploegert S, Demougin P, Heberer M, et al. Three-dimensional culture of melanoma cells profoundly affects gene expression profile: a high density oligonucleotide array study. J.Cell.Physiol. 2005 Aug;204(2):522-531.

(12) Kulesa PM, Fraser SE. Cell dynamics during somite boundary formation revealed by time-lapse analysis. Science 2002 Nov 1;298(5595):991-995.

(13) Hove JR, Koster RW, Forouhar AS, Acevedo-Bolton G, Fraser SE, Gharib M. Intracardiac fluid forces are an essential epigenetic factor for embryonic cardiogenesis. Nature 2003 Jan 9;421(6919):172-177.

(14) Microfluidic control of stem cell diffusible signaling. Micro Total Analysis Systems: Kluwer Academic Pub; 2008.

(15) Chung S, Sudo R, Mack PJ, Wan CR, Vickerman V, Kamm RD. Cell migration into scaffolds under co-culture conditions in a microfluidic platform. Lab.Chip 2009 Feb;9(2):269-275.

(16) Slager HG, Freund E, Buiting AM, Feijen A, Mummery CL. Secretion of transforming growth factor-beta isoforms by embryonic stem cells: isoform and latency are dependent on direction of differentiation. J.Cell.Physiol. 1993 Aug;156(2):247-256.

(17) Melamed MR, Lindmo T, Mendelsohn ML. Flow Cytometry and Sorting. 2nd ed. New York: Wiley; 1994.

(18) de Jager W, Prakken BJ, Bijlsma JW, Kuis W, Rijkers GT. Improved multiplex immunoassay performance in human plasma and synovial fluid following removal of interfering heterophilic antibodies. J.Immunol.Methods 2005 May;300(1-2):124-135.

(19) Dunbar SA. Applications of Luminex xMAP technology for rapid, high-throughput multiplexed nucleic acid detection. Clin.Chim.Acta 2006 Jan;363(1-2):71-82.

(20) Self CH. Enzyme amplification--a general method applied to provide an immunoassisted assay for placental alkaline phosphatase. J.Immunol.Methods 1985 Feb 11;76(2):389-393.

(21) Wild D. The Immunoassay Handbook. 3rd ed. Oxford, UK: Elsevier Ltd.; 2005.

(22) Mason JT, Xu L, Sheng ZM, O'Leary TJ. A liposome-PCR assay for the ultrasensitive detection of biological toxins. Nat.Biotechnol. 2006 May;24(5):555-557.

(23) Nam J, Thaxton CS, Mirkin CA. Nanoparticle-Based Bio-Bar Codes for the Ultrasensitive Detection of Proteins. Science 2003 September 26;301(5641):1884-1886.

(24) Galopin E, Beaugeois M, Pinchemel B, Camart JC, Bouazaoui M, Thomy V. SPR biosensing coupled to a digital microfluidic microstreaming system. Biosens.Bioelectron. 2007 Dec 15;23(5):746-750.

(25) Burg TP, Godin M, Knudsen SM, Shen W, Carlson G, Foster JS, et al. Weighing of biomolecules, single cells and single nanoparticles in fluid. Nature 2007 04/26;446(7139):1066-1069.

(26) Wu G, Datar RH, Hansen KM, Thundat T, Cote RJ, Majumdar A. Bioassay of prostate-specific antigen (PSA) using microcantilevers. Nat Biotech 2001 09//print;19(9):856-860.

(27) Zheng G, Patolsky F, Cui Y, Wang WU, Lieber CM. Multiplexed electrical detection of cancer markers with nanowire sensor arrays. Nat Biotech 2005 10//print;23(10):1294-1301.

(28) Wang Y, - Han J. Pre-binding dynamic range and sensitivity enhancement for immuno-sensors using nanofluidic preconcentrator. Lab on a Chip (3):392.

(29) Jemere AB, Oleschuk RD, Ouchen F, Fajuyigbe F, Harrison DJ. An integrated solid-phase extraction system for sub-picomolar detection. Electrophoresis 2002 Oct;23(20):3537-3544.

(30) Li Y, DeVoe DL, Lee CS. Dynamic analyte introduction and focusing in plastic microfluidic devices for proteomic analysis. Electrophoresis 2003 Jan;24(1-2):193-199.

(31) Beard NP, Zhang C, deMello AJ. In-column field-amplified sample stacking of biogenic amines on microfabricated electrophoresis devices. Electrophoresis 2003;24(4):732-739.

(32) Wainright A, Williams SJ, Ciambrone G, Xue Q, Wei J, Harris D. Sample pre-concentration by isotachophoresis in microfluidic devices. Journal of Chromatography A, 2002 12/6;979(1-2):69-80.

(33) Y. C. Wang. Electrokinetic Trapping of Biomolecules:Novel Nanofluidic Devices for Proteomic ApplicationsMassachusetts Institute of Technology; 2007.

(34) Rubinstein SM, Manukyan G, Staicu A, Rubinstein I, Zaltzman B, Lammertink RG, et al. Direct observation of a nonequilibrium electro-osmotic instability. Phys.Rev.Lett. 2008 Dec 5;101(23):236101.

(35) Wang Y-, Stevens AL, Han J. Million-fold Preconcentration of Proteins and Peptides by Nanofluidic Filter. Anal. Chem. 2005;77(14):4293-4299.

(36) Lee JH, Song Y, Han J. Multiplexed proteomic sample preconcentration device using surface-patterned ion-selective membrane. Lab on a Chip 2008:-.

(37) Di Carlo D, Aghdam N, Lee LP. Single-Cell Enzyme Concentrations, Kinetics, and Inhibition Analysis Using High-Density Hydrodynamic Cell Isolation Arrays. Anal.Chem. 2006 07/01;78(14):4925-4930.

(38) Kim SJ, Wang YC, Lee JH, Jang H, Han J. Concentration polarization and nonlinear electrokinetic flow near a nanofluidic channel. Phys.Rev.Lett. 2007 Jul 27;99(4):044501.

(39) Jin X, Joseph S, Gatimu EN, Bohn PW, Aluru NR. Induced electrokinetic transport in micro-nanofluidic interconnect devices. Langmuir 2007 Dec 18;23(26):13209-13222.

(40) Dhopeshwarkar R, Crooks RM, Hlushkou D, Tallarek U. Transient effects on microchannel electrokinetic filtering with an ion-permselective membrane. Anal.Chem. 2008 Feb 15;80(4):1039-1048.

(41) Isumi Y, Minamino N, Kubo A, Nishimoto N, Yoshizaki K, Yoshioka M, et al. Adrenomedullin stimulates interleukin-6 production in Swiss 3T3 cells. Biochem.Biophys.Res.Commun. 1998 Mar 17;244(2):325-331.